A genome-wide association study uncovers a *ZmRap2.7-ZCN9/ZCN10* module to regulate ABA signalling and seed vigour in maize

Shasha Guo[1,†], Junmin Ai[1,†], Nannan Zheng[1], Hairui Hu[1], Zhuoyi Xu[1], Quanquan Chen[1], Li Li[1], Yunjun Liu[2] (iD), Hongwei Zhang[2], Jieping Li[3], Qingchun Pan[3] (iD), Fanjun Chen[3], Lixing Yuan[3] (iD), Junjie Fu[2] (iD), Riliang Gu[1,4,*], Jianhua Wang[1,*] and Xuemei Du[1,*] (iD)

[1]State Key Laboratory of Maize Bio-breeding, Beijing Innovation Center for Crop Seed Technology (MOA), College of Agronomy and Biotechnology, China Agricultural University, Beijing, China

[2]Institute of Crop Science, Chinese Academy of Agricultural Sciences, Beijing, China

[3]State Key Laboratory of Nutrient Use and Management, College of Resources and Environmental Sciences, National Academy of Agriculture Green Development, China Agricultural University, Beijing, China

[4]Joint Research Institute of China Agricultural University in Aksu, Aksu, China

Summary

Seed vigour, including rapid, uniform germination and robust seedling establishment under various field conditions, is becoming an increasingly essential agronomic trait for achieving high yield in crops. However, little is known about this important seed quality trait. In this study, we performed a genome-wide association study to identify a key transcription factor *ZmRap2.7*, which regulates seed vigour through transcriptionally repressing expressions of three ABA signalling genes *ZmPYL3*, *ZmPP2C* and *ZmABI5* and two phosphatidylethanolamine-binding genes *ZCN9* and *ZCN10*. In addition, ZCN9 and ZCN10 proteins could interact with ZmPYL3, ZmPP2C and ZmABI5 proteins, and loss-of-function of *ZmRap2.7* and overexpression of *ZCN9* and *ZCN10* reduced ABA sensitivity and seed vigour, suggesting a complex regulatory network for regulation of ABA signalling mediated seed vigour. Finally, we showed that four SNPs in *ZmRap2.7* coding region influenced its transcriptionally binding activity to the downstream gene promoters. Together with previously identified functional variants within and surrounding *ZmRap2.7*, we concluded that the distinct allelic variations of *ZmRap2.7* were obtained independently during maize domestication and improvement, and responded separately for the diversities of seed vigour, flowering time and brace root development. These results provide novel genes, a new regulatory network and an evolutional mechanism for understanding the molecular mechanism of seed vigour.

Introduction

In the coming decades, maintaining a steady food supply for the increasing world population will require high-yielding crop plants which can be productive under various environments (Saatkamp *et al.*, 2019). Maintaining high yields requires successful seed germination and uniform seedling establishment in fields (Rajjou *et al.*, 2012; Saatkamp *et al.*, 2019). Seed vigour, a complex agronomic trait that includes germination speed, seedling growth and early stress tolerance, determines the success of this establishment (Rajjou *et al.*, 2012; Zhou *et al.*, 2020). For crop seeds, their vigour is usually obtained at the physiological maturity, and then continuously lost due to post-harvest deterioration during storage (Rajjou *et al.*, 2012; Zhou *et al.*, 2020). Thus, maintenance of seed vigour during storage, which is generally called as seed longevity, is critical for high-yield production of crops (Zhou *et al.*, 2020).

Maize production annually requires more than two-billion-kilogram seeds (Erenstein *et al.*, 2022). Compared with other cereals, maize seed is relatively sensitive to storage deterioration, as it has no dormancy strategy and its embryo is large with high oil concentration (Xue *et al.*, 2021). Accelerated ageing (AA) test is a method widely adopted for predicting seed vigour after storage in maize (Bueso *et al.*, 2013; Liu *et al.*, 2019). Based on this method, reverse genetics identified three genes regulating seed longevity from maize (Han *et al.*, 2020; Li *et al.*, 2017; Zhang *et al.*, 2023). The first one encoded a raffinose synthase (ZmRS/ZmRAFS) that could decrease sugar content and prolong seed longevity (Li *et al.*, 2017), and the second was a dehydration-responsive element-binding2a (ZmDREB2A) transcription factor that functions in upstream of *ZmRAFS* (Han *et al.*, 2020). The third one was ZmPIMT2 that interacts with mitochondrial protein 3-methylcrotonyl CoA carboxylase (ZmMCC) to repair abnormal isoaspartyl damage, and positively

regulates seed longevity (Zhang et al., 2023). Meanwhile, dozens of quantitative trait loci (QTL) relating to seed longevity have been identified from maize (Liu et al., 2019; Reed et al., 2022; Wang et al., 2016), but none of the underlying genes has been cloned.

Studies from Arabidopsis and rice have revealed several genes encoding protective compounds that could protect seed from deterioration and prolong longevity in plants (Li et al., 2017; Zhou et al., 2020; Zinsmeister et al., 2020). Meanwhile, genes functioning in ROS eliminating, protein-repairing and genome stability maintaining have also been proved to participate in prolonging seed vigour after storage (Châtelain et al., 2013; Chen et al., 2016; Ogé et al., 2008; Waterworth et al., 2016). Recently, abscisic acid (ABA), a vital hormone regulating seed germination and dormancy, was proven to regulate seed vigour after storage, probably through targeting genes encoding protective compounds and repairing proteins (Zhou et al., 2020). ABA signal transduction contains four components: pyrabactin resistance (PYR)-like (PYL)/regulatory component of ABA receptor (RCAR) receptors, protein phosphatase 2C (PP2C) co-receptors, SNF1-related kinase 2 s (SnRK2) and ABA-responsive element (ABRE)-binding proteins (AREB)/ABRE-binding factor (ABF) transcription factors (Cutler et al., 2010; Weiner et al., 2010). Within these components, at least three ABFs, transcription factor ABA-insensitive 3 (ABI3), ABI4 and ABI5, were revealed to regulate seed longevity through targeting protective compounds of late embryogenesis abundant proteins (LEAs) and raffinose family oligosaccharides (RFOs), and protein-repairing proteins (Clerkx et al., 2003; Kamble et al., 2022; Mao and Sun, 2015; Tian et al., 2020; Zinsmeister et al., 2016). These results indicated that ABA signalling mediated protection and repairing systems are associated with seed vigour after storage. However, the upstream regulators of ABA signalling were largely unknown in plants.

In this study, we conducted a genome-wide association study (GWAS) to identify a key transcription factor ZmRap2.7 for regulating maize seed vigour after storage, and uncovered its regulatory mechanism involving in transcriptionally repressing expressions of three ABA signalling genes *ZmPYL3*, *ZmPP2C* and *ZmABI5* and two phosphatidylethanolamine-binding genes *ZCN9* and *ZCN10*, and interactions between the two group proteins. Then, the allelic variants in *ZmRap2.7* coding region were investigated to illustrate the trait evolution of seed vigour during maize domestication and improvement. These results provide novel genes and regulatory networks for understanding the molecular mechanism of seed vigour.

Results

GWAS for maize seed vigour after accelerated ageing

As seed quality is greatly affected by maternal growth environments, we planted a maize association population, containing 368 inbred lines (Fu et al., 2013), in 3 years to minimize this effect. In addition, to eliminate lower quality seeds that were possibly raised from stressed maternal growth environments, we conducted standard germination (SG) test, a method widely adopted for determining the highest germination potential at ideal germination conditions (ISTA, 2015), and selected lines with SG percentage higher than 80% for AA test. Finally, seeds from 217, 291 and 194 lines harvested in 2011, 2016 and 2017, respectively, were subjected to 3-day AA treatment (AA3). Germination test of the aged seeds showed large variations for AA3 germination percentage (AA3-GP; from 32.0% to 98.7%),

with a broad sense heritability of 0.54 (Table S1; Figure 1a). The coefficient of variation for AA3-GP among lines ranged from 21% to 24% in different produce years, and the correlation coefficients between years ranged from 0.26 to 0.40 (Table S1).

Using the average phenotypic value from 3 years and 553 906 SNPs with a minor allele frequency (MAF) of ≥0.05 (Fu et al., 2013), we performed GWAS to identify genetic loci underlying AA3-GP. After inputting the population structure (Q) and kinship (K) matrices into a mixed linear model (MLM) to control false positives, four SNPs were identified significantly associating with AA3-GP at a significance level of $-\log_{10}(P) \geq 5.70$ ($P \leq 1$/effective SNP number (EN) = 1.81×10^{-6}; EN is 553 906) (Figure 1b). The four SNPs are in strong linkage disequilibrium (LD) and are in exons of *GRMZM2G700665* on chromosome 8, with one in the first exon and three in the seventh exon (Figure 1c,d). The lead SNP explained ~9% phenotypic variation for AA3-GP (Table S2).

We screened each 100 kb region upstream and downstream from the lead SNP and identified five protein-coding genes (Figure 1d). The expression levels of these genes were investigated in embryos that were collected at 24 h after AA3 germination by quantitative polymerase chain reaction (qPCR). The results showed that *GRMZM2G700665* was the only highly expressed gene in AA3 germinated embryos (Figure 1e), suggesting it as a putative candidate gene underlying maize seed vigour.

ZmRap2.7 is significantly associated with seed vigour after accelerated ageing

GRMZM2G700665 encodes an AP2-type transcription factor ZmRap2.7, a well-known protein previously identified for regulating flowering time in maize (Liang et al., 2019; Salvi et al., 2007). To explore its functions in regulating seed vigour, we firstly investigated its expressions in different maize tissues and found that it is constitutively expressed in all investigated tissues, with the highest level in 24-h AA3 germinated embryos (Figure 2a). After AA treatment for 1–6 days, *ZmRap2.7* expression showed no significant change compared to dry seeds (Figure 2b). However, during AA3 germination, its expression increased from 0 to 24 h after imbibition, and then dropped from 24 h to 72 h (Figure 2b). During SG germination, its expression showed a similar change trend to AA3 germination, but the peak moved to 12 h (Figure S1). *In situ* hybridization revealed that *ZmRap2.7* mainly expressed in embryo and aleurone layer, but not in endosperm (Figure 2c). These expression patters were consistent with the previous conclusion that embryo and aleurone layer were the main tissues relating to seed vigour after storage (Li et al., 2019b; Zhang and Ogas, 2009).

To clarify the role of *ZmRap2.7* in seed vigour, two *ZmRap2.7* transgenic knockout lines *ZmRap2.7*-KO#1 and *ZmRap2.7*-KO#2 in B73 background, generated in a previous work (Liang et al., 2019), were used for germination test. No GP differences were observed between knockout lines and wild type (WT; B73) under SG condition (Figure 2d). However, under AA3 condition, the GP of *ZmRap2.7*-KO#1 and KO#2 decreased to 19.3% and 17.8%, respectively, while that of WT was 56.7% (Figure 2d). Under AA6 (accelerated ageing for 6 days), the GP of *ZmRap2.7*-KO#1 and KO#2 decreased to 1.3% and 3.0%, respectively, while that of WT was 10.0% (Figure 2d). Moreover, a Mu insertion mutant of *ZmRap2.7* (*ZmRap2.7*-Mu) in W22 background, isolated in a previous work (Li et al., 2019a), also showed significantly lower GP than WT (W22) under both AA3 and AA6 conditions, but showed comparable GP to WT under SG condition (Figure S2). These results
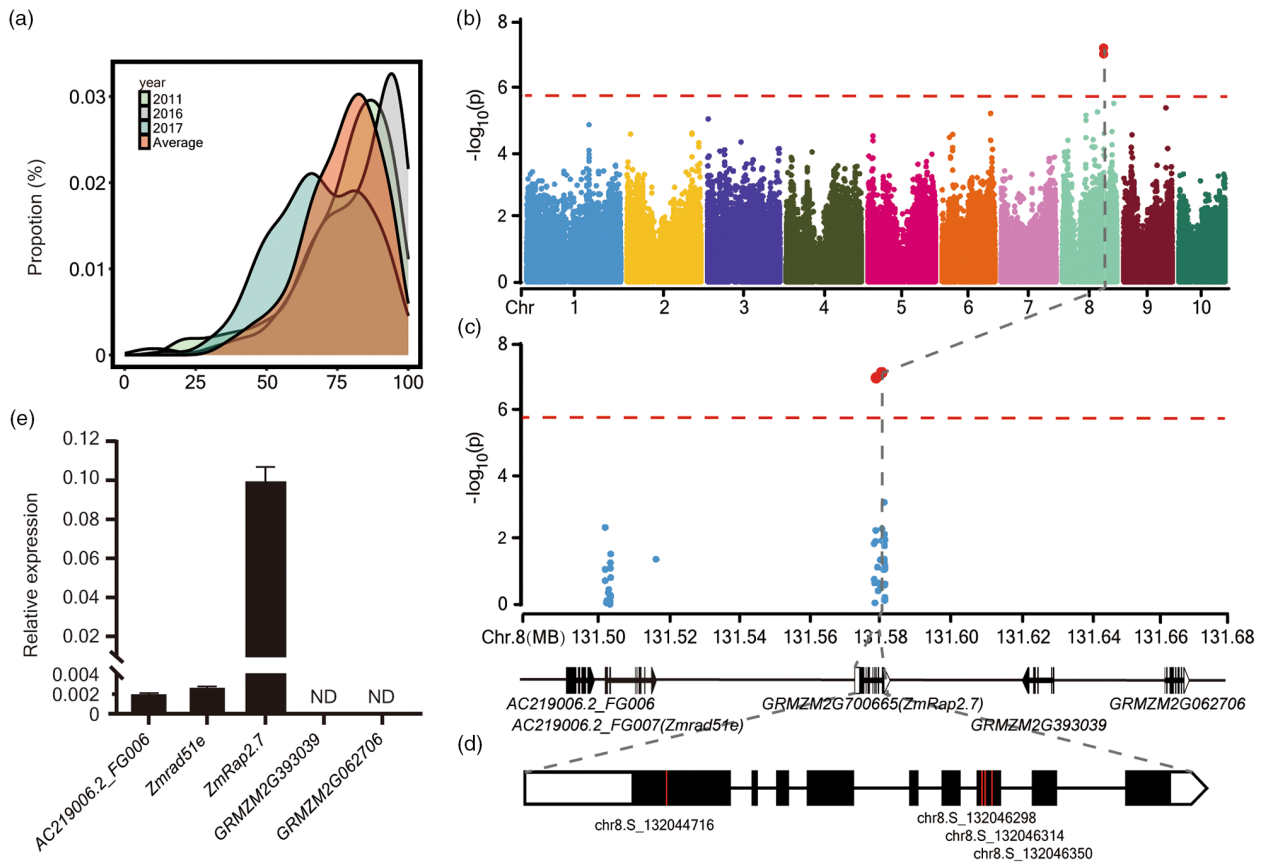
Figure 1 GWAS for seed vigour after accelerated ageing. (a) Variation of seed germination percentage after 3 days of accelerated ageing treatment (AA3-GP) in an association population containing 368 lines. Seeds were harvested in 2011, 2016 and 2017. (b) Manhattan plot of GWAS for AA3-GP. The dashed horizontal line indicates the significance threshold ($-\log_{10} (P) \geq -\log_{10}$(1/effective SNP number (EN)); EN=533906)). (c) Local Manhattan plot (each 100-kb region upstream and downstream from the lead SNP) showing the GWAS peak on chromosome eight and the five protein-coding genes in this region according to the B73 reference genome (RefGen_v3). Four significant SNPs are highlighted by red dots. (d) Gene structure of *GRMZM2G700665* (*ZmRap2.7*). Red vertical lines represent the location of the four significant SNPs in this gene. (e) Expression levels of the five protein-coding genes in the embryos collected at 24 h after AA3 germination by quantitative polymerase chain reaction (qPCR). GAPDH was used as an internal control and the error bars indicate mean $\pm$ SD ($n = 3$). ND, not detected.

suggested that loss-of-function of *ZmRap2.7* decreases seed AA-GP.

ZmRap2.7 transcriptionally represses ABA signalling genes *ZmPYL3*, *ZmPP2C* and *ZmABI5*

To explore the regulatory network for *ZmRap2.7*-mediated seed vigour, we performed RNA-seq analysis of embryos collected at 24 h after AA3 germination. Compared with WT, 1750 differentially expressed genes (DEGs), including 708 down-regulated and 1042 up-regulated, were identified from *ZmRap2.7*-KO#1 using thresholds of FDR <0.05 and $\log_2$(|fold change|) ≥ 1 (Figure 3a, Table S4). Gene ontology (GO) analysis of these DEGs revealed that the most significantly enriched term was a response to hormone stimulus (GO:0009752) (Figure 3b). This term included 69 DEGs with eight up-regulated DEGs involved in ABA signalling pathway, including one *PYL*, five *PP2Cs* and two *ABFs* (Figure 3c). The DEGs also included 11 up-regulated genes for ABA-responsive genes. The expression levels of these 19 ABA-related genes were further verified in WT and KO lines by qPCR, and the results showed similar trends with the RNA-seq results (Figure 3d; Figure S3).

To further uncover the regulatory relationship between ZmRap2.7 protein and the eight ABA signalling DEGs, we amplified ~1 kb (relating to the translation start site ATG) promoter sequences for one-hybrid (Y1H) assay. The results showed that ZmRap2.7 protein could interact with three out of the eight DEG promoters, that is, *ZmPYL3*, *ZmPP2C* and *ZmABI5* (an *ABF* gene) (Figure 3e; Figure S4a). Furthermore, we divided these promoters into different fragments, and Y1H assay showed that ZmRap2.7 interacted with "*ZmPYL3-a*" (from -1001 bp to -808 bp relating to ATG), "*ZmPYL3-b*" (from -807 bp to -580 bp), "*ZmPP2C-a*" (from -474 bp to -199 bp), "*ZmPP2C-b*" (from -198 bp to -102 bp) and "*ZmABI5-b*" (from -247 bp to -125 bp) fragments (Figure S4b,c).

Then, we conducted an electrophoretic mobility shift assay (EMSA) to investigate the *in vitro* binding between ZmRap2.7 protein and each of "*ZmPYL3-a*", "*ZmPP2C-a*" and "*ZmABI5-b*" fragments (Figure 3f). The results showed that each fragment formed DNA–protein complex migrated slower than the non-bound DNA in native polyacrylamide gels, and the DNA–protein complexes became weak when unlabelled compete probes were added (Figure 3f). Together with the increased
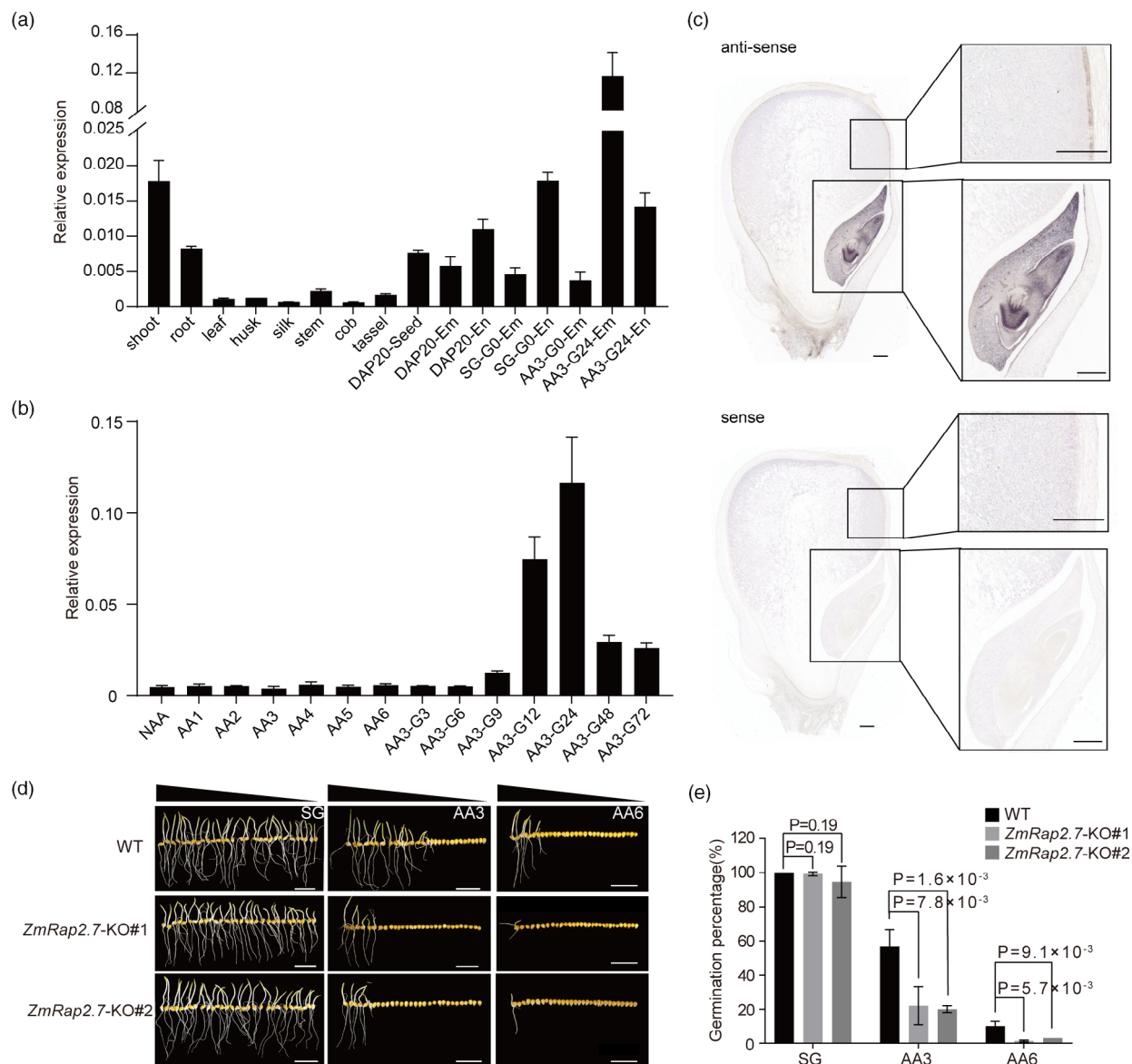
Figure 2 *ZmRap2.7* is significantly associated with seed vigour after accelerated ageing. (a) *ZmRap2.7* expression in different maize organs. AA3, 3-day accelerated ageing germination; DAP, days after pollination; Em, embryo; En, endosperm; G0, 0 h after imbibition; G24, 24 h after imbibition; SG, standard germination. (b) *ZmRap2.7* expression in embryos during AA treatment from 0 to 6 days, and AA3 germination from 0 to 72 h after imbibition. GAPDH was used as an internal control and the error bars indicate mean $\pm$ SD ($n = 3$). (c) *In situ* hybridization of *ZmRap2.7* gene in 18 DAP kernel. The sense and antisense sequence of *ZmRap2.7* were used as hybridization probes. Bars = 0.5 mm. (d) Germination performance of *ZmRap2.7*-KO lines and their WT (B73) at SG, AA3 and AA6 (6-day accelerated ageing germination) conditions. Bars = 5 cm. (e) Germination percentage of seeds in (d). Data were collected at 7 days after imbibition. Values are means $\pm$ SD ($n = 3$).

expressions of *ZmPYL3*, *ZmPP2C* and *ZmABI5* in *ZmRap2.7* KO lines (Figure 3d,e), these results suggested that ZmRap2.7 could directly bind to these three ABA signalling gene promoters to transcriptionally repress their expressions.

Loss-of-function of *ZmRap2.7* decreased ABA sensitivity during seed germination

As ZmRap2.7 could bind to ABA signalling gene promoters, we conducted exogenous ABA treatment to WT and *ZmRap2.7*-KO lines. Before treatment, AA3-GPs of *ZmRap2.7*-KO#1 (30.7%) and *ZmRap2.7*-KO#2 (32.0%) were significantly lower than that of WT (64.0%, Figure 3h). However, after treatment, both KO

lines showed comparable AA3-GP to WT (Figure 3g,h), indicating less reductions of AA3-GP in KO lines than in WT by ABA treatment (Figure 3g,h). The less reduction of SG percentage in KO lines than in WT was also observed by ABA treatment (Figure S5). These results indicated that loss-of-function of *ZmRap2.7* decreased ABA sensitivity during seed germination.

We further detected the changes of *ZmRap2.7*, *ZmPYL3*, *ZmPP2C* and *ZmABI5* expressions in response to ABA treatment. Compared to mock experiments, ABA treatment decreased *ZmRap2.7* expression in AA3 germinated WT embryos (Figure S6). For the ABA signalling genes, ABA treatment reduced *ZmPYL3* expressions in both WT and KO lines, but the reduction

levels were less in KO lines (50.1%–53.5%) than in WT (80.7%; Figure 3i). Meanwhile, ABA induced *ZmPP2C* expression, and the increased levels in KO lines (40.3%–81.7%) were less than in WT (96.1%; Figure 3j). ABA dramatically induced *ZmABI5* expression in WT, while slightly repressed its expressions in KO lines (Figure 3k). Taken together, these results suggested that loss-of-function of *ZmRap2.7* attenuated changes of *ZmPYL3*, *ZmPP2C* and *ZmABI5* expressions in response to ABA treatment.

ZmRap2.7 transcriptionally represses *ZCN9* and *ZCN10* expressions

Previous work showed that *ZmRap2.7* negatively regulates the *FT/ZCN8* gene expression to postpone flowering time (Liang et al., 2019). *ZCN8* belongs to a phosphatidylethanolamine-binding protein (PEBP) family that contains three subfamilies, FT, FTL (flowering time like) and MFT (mother of FT and FTL) (Danilevskaya et al., 2008). Among them, MFT subfamily has been reported to be expressed exclusively in seeds (Nakamura et al., 2011; Song et al., 2020; Xi et al., 2010). Therefore, we asked whether MFT subfamily members being the potential targets of ZmRap2.7 in maize seeds.

To answer this question, we conducted qPCR to investigate expressions of the three previously identified MFT genes, *ZCN9*, *ZCN10* and *ZCN11* (Danilevskaya et al., 2008), in *ZmRap2.7*-KO lines. The results showed that *ZCN9* and *ZCN10* expressions in AA3 germinated embryos of *ZmRap2.7*-KO#1 were three and nine times higher than those of WT, respectively (Figure 4a), but *ZCN11* expression did not change by *ZmRap2.7* knockout (Figure S7). Furthermore, we performed a comparative genome analysis to show that *ZCN9* and *ZCN10* were a pair of syntenic homologues, and might have been recently duplicated by the specific whole genome duplication of maize (commonly named allotetraploidization) (Figure S8). However, *ZCN11* was not a syntenic homologue of *ZCN9* and *ZCN10*. These results suggested that *ZCN9* and *ZCN10*, but not *ZCN11*, were syntenic homologues that might have similar expressions regulated by *ZmRap2.7*.

Then, we focused on *ZCN9* and *ZCN10* and found that both were exclusively expressed in seeds with the highest levels in embryos (Figure S9a,d). In embryos, both gene expressions decreased dramatically after imbibition during AA3 germination (Figure S9b,e), which was opposite to the *ZmRap2.7* expression. *In situ* hybridization was carried out to reveal that both *ZCN9* and *ZCN10* are mainly expressed in embryo and aleurone layer, which was similar to the *ZmRap2.7* expression (Figure S9c,f). These results suggested that *ZCN9* and *ZCN10* expressions in embryo and aleurone might be repressed by ZmRap2.7 during AA3 germination.

To explore the regulatory mechanism of *ZCN9* and *ZCN10* expressions by *ZmRap2.7*, we performed Y1H assay and found that ZmRap2.7 protein could bind to ~1 kb promoter (relating to ATG) of both *ZCN9* and *ZCN10* genes. After dividing the promoter into several fragments (Figure 4b), we found that ZmRap2.7 displayed strong binding to the "a" (−345 to −1 bp; *ZCN9*-a), and "b" (−720 bp to −470 bp; *ZCN10*-b) fragments of *ZCN9* and *ZCN10* promoters respectively (Figure 4c). We further divided the "*ZCN9*-a" and "*ZCN10*-b" into several segments, and conducted EMSA assays to find that 6His-tagged ZmRap2.7 protein was capable of binding both "a1" and "a2" segments of *ZCN9* promoter *in vitro* (Figure S10a). As "a1" and "a2" segments had 20 bp sequence overlapped, we synthesized another probe "a3" (−195 bp to −234 bp) that covered this

overlapped sequence and found that this probe could be bonded by ZmRap2.7 (Figure 4d). For *ZCN10* promoter, the results showed that ZmRap2.7 bonded to the "b1" segment (−591 bp to −630 bp; Figure 4d), but not to the others (Figure S10b). In addition, these binding bonds could be competed off by 10 and 40 times unlabelled probes (Figure 4d). Together with the attenuated decreases of *ZCN9* and *ZCN10* expressions in *ZmRap2.7* knockout lines (Figure 4a), Y1H and EMSA assays demonstrated that ZmRap2.7 could directly bind to both gene promoters and repress their expressions.

To survey the roles of *ZCN9* and *ZCN10* in seed vigour, we generated transgenic overexpression (OE) lines (*ZCN9*-OE#1 and *ZCN9*-OE#2, *ZCN10*-OE#1 and *ZCN10*-OE#2) driven by a ubiquitin promoter in CAL background (Du et al., 2019). qPCR analysis showed that the expressions of both genes were elevated in OE lines by 3–70 times (Figure 4e,h). The SG percentage of *ZCN9*-OE and *ZCN10*-OE lines was close to 100%, which was similar to those of WT (CAL; Figure 4f,g,i,j). However, the AA3-GP of *ZCN9*-OE#1 and *ZCN9*-OE#2 decreased to 84.7% and 74.0%, respectively, and *ZCN10*-OE#1 and *ZCN10*-OE#2 to 63.3% and 68.0%, respectively, while those of WT maintained at 92.0% (Figure 4f,g,i,j). These results indicated that *ZCN9* and *ZCN10* were negative regulators of seed vigour after accelerated ageing.

ZCN9 and ZCN10 interact with ZmPYL3, ZmPP2C and ZmABI5

ZCN9 and ZCN10 belong to the PEBP family, and these family members usually act as partners of nuclear localization protein, such as transcription factor (Song et al., 2020). To explore the possible partner roles of ZCN in ABA signalling pathway, we expressed and purified glutathione S-transferase-tagged ZCN9 (GST-ZCN9), GST-ZCN10 and His 6-tagged ZmABI5 (His-ZmABI5), His-ZmPYL3 and His-ZmPP2C, to perform pull-down assay. After immobilization of GST fused proteins, His-ZmABI5, His-ZmPYL3 and His-ZmPP2C could be detected in the pull-down products (Figure 5a–c), indicating that these three proteins could interact with ZCN9 and ZCN10 *in vitro*. Furthermore, luciferase complementation image (LCI) and bimolecular fluorescence complementation (BiFC) assay in the leaves of N. *benthamiana* confirmed all these six pairs of interaction (Figure 5d–i). BiFC assays also showed that these interactions occurred in nucleus (Figure 5g–i). These results concluded that both ZCN9 and ZCN10 can directly interact with ZmPYL3, ZmPP2C and ZmABI5.

To further clarify the roles of *ZCN9* and *ZCN10* in ABA signalling during seed AA germination, we conducted ABA treatment to their transgenic OE lines (Figure S11). Compared to mock experiments, ABA treatment decreased AA3-GP of WT by 69.6%–72.5%; while decreased those of *ZCN9* and *ZCN10* OE lines only by 10.0%–12.5% (Figure S11). These results suggested that overexpression of *ZCN9* and *ZCN10* could decrease ABA sensitivity during seed AA germination, which is similar to *ZmRap2.7* KO lines.

Variations in nonsynonymous substitutions confer ZmRap2.7 different transcription activity

To uncover the functional variation of *ZmRap2.7*, we extracted ZmRap2.7 genome sequences from public genome data of the AM368 population for SNP calling (Yang et al., 2019), and found 177 SNPs having minor allele frequencies (MAF) ≥0.05 in the genome of *ZmRap2.7*. Then, we re-sequenced *ZmRap2.7* genome sequence and found a presence/absence variation (PAV) in −813 bp upstream of the ATG (Figure 6a). Together

with the classical MITE insertion variant in ~70-kb upstream of *ZmRap2.7* (Castelletti *et al.*, 2014; Salvi *et al.*, 2007), candidate gene association analysis revealed that the GWAS identified four

SNPs showed the most significant association with AA3-GP again, while the MITE insertion and promoter PAV showed much higher *P* values than the four SNPs (Figure 6a). These four SNPs are
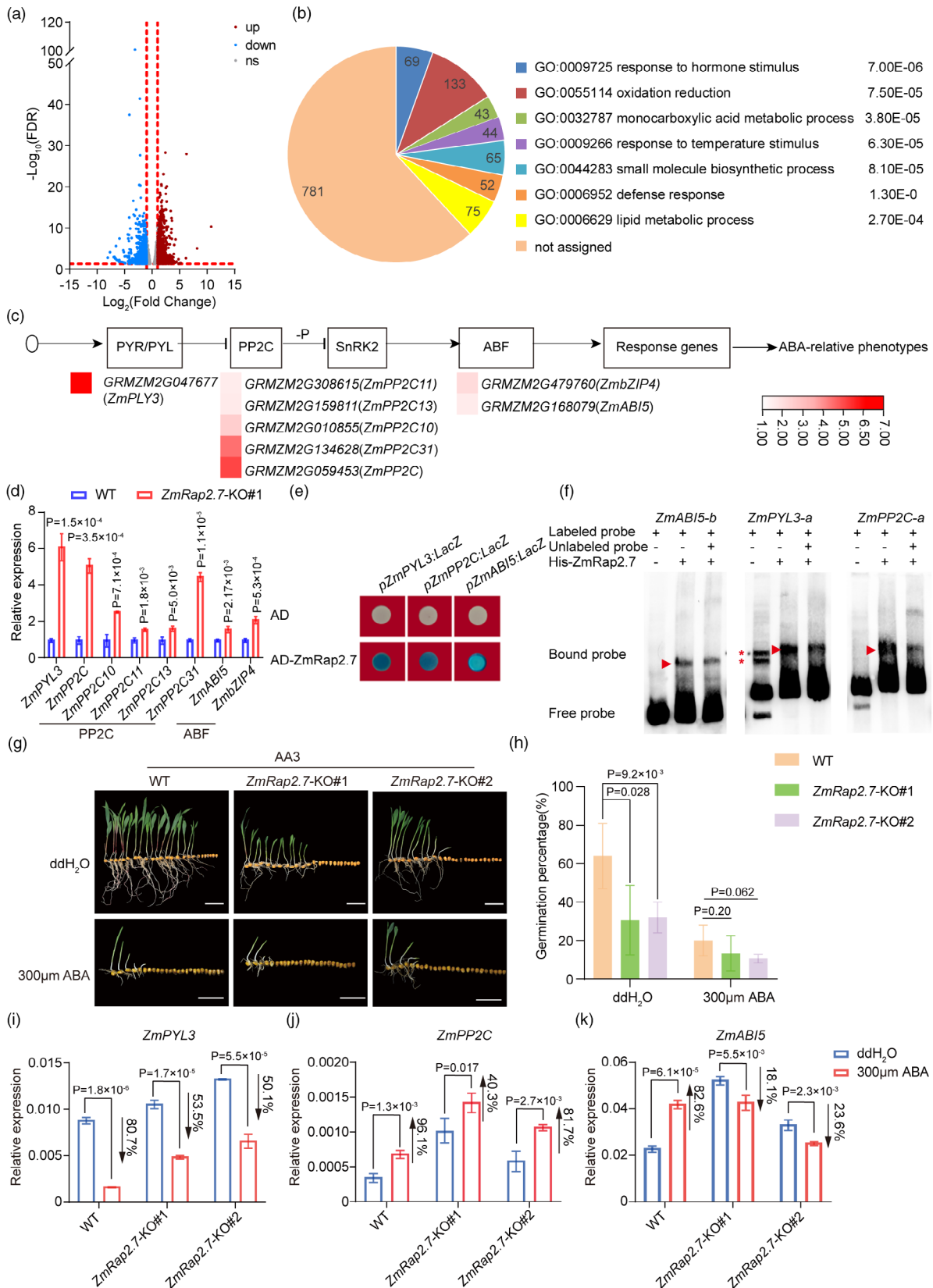
Figure 3 ZmRap2.7 transcriptionally represses expressions of ABA signalling gene *ZmPYL3*, *ZmPP2C* and *ZmABI5*. (a) Volcano plot representing the differentially expressed genes (DEGs) between *ZmRap2.7*-KO#1 and wild type (WT) embryos collected at 24 h after imbibition of 3-day accelerated ageing germination (AA3). Blue and red represent down-regulated and up-regulated genes respectively. (b) GO functional analysis of the DEGs. (c) The up-regulated DEGs involving in ABA signalling. (d) The relative expression levels of the ABA signalling genes in 24-h AA3 germinated embryos of *ZmRap2.7*-KO#1 and WT. (e) Yeast one-hybrid (Y1H) assays showing interactions between ZmRap2.7 protein and *ZmPYL3*, *ZmPP2C* and *ZmABI5* promoters. AD was the empty vector as a negative control, and AD-ZmRap2.7 represented *ZmRap2.7* gene fused to the pB42AD vector. (f) EMSA assays showing ZmRap2.7 protein interacted with the promoters "*ZmPYL3*-a" (from −1001 bp to −808 bp relating to ATG), "*ZmPP2C*-a" (from −474 bp to −199 bp) and "*ZmABI5*-b" (from −247 bp to −125 bp) fragments *in vitro*. The probe sequences are listed in Table S3. (g) AA3 germination performance of WT, *ZmRap2.7*-KO#1 and *ZmRap2.7*-KO#2 by ABA treatment. Bars = 5 cm. (h) Germination percentage of seeds in (g). Data were collected at 10 and 7 days after imbibition of ABA treatment and none-treatment respectively. Values are means ± SD (*n* = 3). (i–k) Expression level of *ZmPYL3* (i), *ZmPP2C* (j) and *ZmABI5* (k) in *ZmRap2.7*-KO#1 and WT at 24 h after imbibition of AA3 germination by ABA treatment. GAPDH was used as an internal control. Arrows indicated ranges of expression change after ABA treatment compared to the mock treatment.

located in exon of *ZmRap2.7*, indicating that the coding sequence of *ZmRap2.7* might control the phenotypic variation of AA3-GP.

To test this hypothesis, we grouped the 368 population lines into four haplotype groups according to the four significant SNPs and found that haplotype 1 (Hap1) was the largest group containing 299 lines, and Hap2 was the second largest group containing 16 lines. Hap3 and Hap4 were minor groups, comprising two and one lines respectively (Figure 6b). Statistically, Hap1 lines had a significantly higher AA3-GP than Hap2 lines (Figure 6c). Then, we analysed *ZmRap2.7* expression levels in AA3 germinated embryos of the 16 Hap2 lines and randomly selected 53 Hap1 lines. The expression levels of the two groups were comparable (Figure S12), indicating that the transcript level was unlikely to be responsible for the functional divergence of *ZmRap2.7* for seed vigour.

Finally, we focused on the transcription activity of ZmRap2.7 protein and conducted a luciferase (LUC) assay to compare the binding activity of ZmRap2.7[Hap1] (from inbred B73) and ZmRap2.7[Hap2] (from CA47) in maize protoplasts. As expression analysis has indicated ZmRap2.7 as a transcription repressor (Figures 3d, 4a), we fused the strong activation domain from viral protein16 (VP16) of the herpes simplex virus to either N or C terminus of ZmRap2.7 proteins for elevating the control LUC activity (Hu *et al.*, 2020). The results showed that the C terminus fused VP16 increased LUC activity more than the N terminus fused (Figure S13). Thus, we used the VP16 C terminus to fuse ZmRap2.7 for activity assays and found that LUC activities in ZmRap2.7[Hap1] and ZmRap2.7[Hap2] fused VP16 were significantly lower than that in VP16 control, supporting the transcription repressing function of both ZmRap2.7 haplotypes (Figure 6d,e). Furthermore, we found that the transcriptional inhibitory activity of ZmRap2.7[Hap1] on the reporter gene was significantly stronger than that of ZmRap2.7[Hap2] (Figure 6e), supporting different repressing activities between these two haplotypes. Then, we detected the expression levels of the five ZmRap2.7′ target genes in AA3 germinated embryos of randomly selected 15 Hap1 lines and 10 Hap2 lines and found that *ZCN9*, *ZCN10*, *ZmPP2C* and *ZmABI5* showed decreased transcription levels in Hap1 lines than in Hap2 lines (Figure S14).

The four SNPs in *ZmRap2.7* resulted in amino acid substitutions at site 64 (Alanine to Valine), 332 (Serine to Arginine), 338 (Pronine to Serine) and 350 (Leucine to Valine) in ZmRap[Hap2] compared with ZmRap[Hap1] (Figure 6d). We further generated single-base mutated CDSs targeting these 4 SNPs in Hap1 background and named as M1–M4 (Figure 6d,f). After C-terminally fusing to VP16, subsequent LUC assays showed that LUC activity of each single-point mutant protein was significantly

higher than that of ZmRap2.7[Hap2], but significantly lower than that of ZmRap2.7[Hap1] (Figure 6e), suggesting that all four substitutions affect transcription repressing activity of ZmRap2.7.

The binding ability between the two haplotypes was further verified by EMSA assay. The results showed that the binding band signals to either ZCN9 or ZCN10 promoter from ZmRap2.7[Hap2] were weaker than those from ZmRap2.7[Hap1] (Figure S15). In addition, the M1–M4 mutant proteins showed a medium binding ability to *ZCN9* promoter between ZmRap2.7[Hap1] and ZmRap2.7[Hap2] (Figure 6f). These results indicated that, compared to ZmRap2.7[Hap1], mutations of the four SNPs in ZmRap2.7 [Hap2] additively decrease its transcriptionally repressing activity on target gene expressions.

The evolution and pleiotropy analysis of *ZmRap2.7* haplotype

We investigated the evolution and selection signature of *ZmRap2.7* using data from HapMap 3 (Bukowski *et al.*, 2018), where we obtained variants in *ZmRap2.7* genome region from 1076 lines, including 18 teosinte, 24 landrace and 1034 improved maize (905 Hap1 and 129 Hap2). Evolution analysis showed that the nucleotide diversity of genomic region covering *ZmRap2.7* showed moderate decrease from teosinte to maize (both landrace and improved maize) (Figure 6g). In maize, the nucleotide diversity was much lower in lines carrying Hap2 than that carrying Hap1 (Figure 6g). In addition, all 18 teosinte accessions carried Hap1 alleles (Table S5). These findings suggested that *ZmRap2.7*[Hap2] might emerged after maize was domesticated from teosinte and underwent strong selection during improvement.

Previous works showed that the insertion of a MITE transposon inhibited the expression of *ZmRap2.7* in cis-form and promoted early flowering (Castelletti *et al.*, 2014); and a single nucleotide substitution located in *ZmRap2.7* gene body (SNP1499) responded for brace root development (Li *et al.*, 2019a). Here, it was interesting to find that the Hap2 only existed in lines with MITE insertion (Figure 6h), and SNP1499-G only existed in lines without MITE insertion (Figure S16). In addition, Hap1 and Hap2 lines showed similar flowering time, that is, heading date, pollen shedding time and silking time within the MITE insertion subpopulation (Figure S17), and similar brace root number (Figure S18). Meanwhile, both MITE insertion and SNP1499 were not associated with seed AA3-GP (Figure 6i,j). These results indicated that the MITE insertion may be selected firstly during domestication, and the four SNPs located in *ZmRap2.7* coding region were selected from the MITE insertion background to depress seed vigour, but not relevant to flowering time and root development.
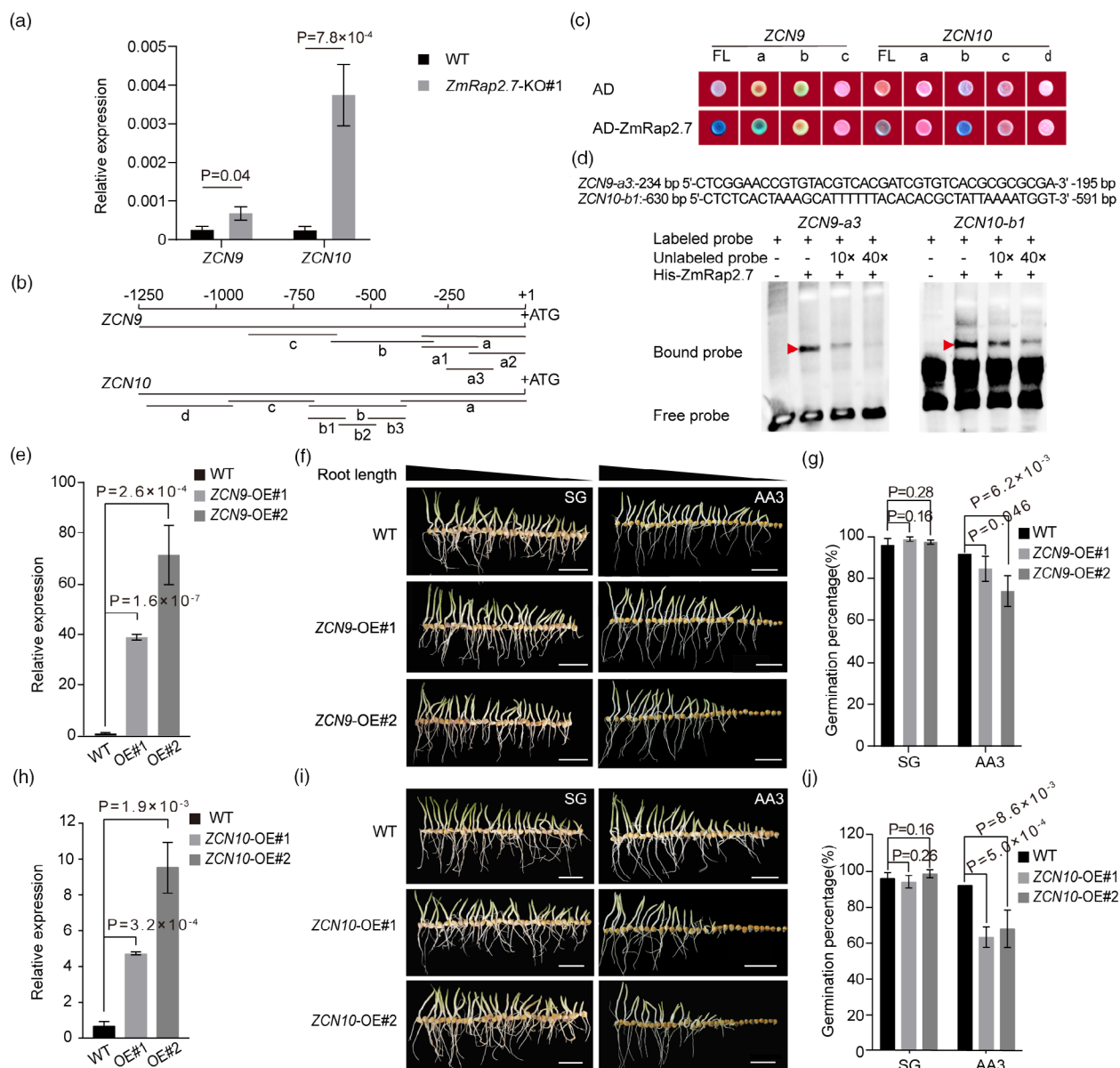
Figure 4 *ZmRap2.7* transcriptionally represses *ZCN9* and *ZCN10* expressions to regulate seed vigour after accelerated ageing. (a) *ZCN9* and *ZCN10* expressions in wild-type (WT) and *ZmRap2.7* knockout line (KO#1). GAPDH was used as an internal control and the error bars indicate mean ± SD (*n* = 3). (b) Diagram of *ZCN9* and *ZCN10* promoter fragments. The translation start codon (ATG) was assigned to position +1. (c) Yeast one-hybrid assays showing ZmRap2.7 binding to the "a" and "b" fragments of *ZCN9* and *ZCN10* promoter respectively. FL, full-length promoter. a–d are the promoter fragments indicated in (b). Empty vector expressing AD domain alone was used as a negative control. (d) EMSA assays showing ZmRap2.7 binding to the "a3" and "b1" segments in *ZCN9* and *ZCN10* promoter *in vitro* respectively. (e and h) *ZCN9* (e) and *ZCN10* (h) expressions in WT and their OE lines. GAPDH was used as an internal control. (f and i) Germination performance of WT (inbred line CAL), *ZCN9*-OE (f) and *ZCN10*-OE (i) lines at standard germination (SG) and 3-day accelerated ageing germination (AA3) conditions. OE, overexpression. Bars = 5 cm. (g and j) Germination percentage of seeds in (f) and (i). Data were collected at 7 days after imbibition. Values are means ± SD (*n* = 3).

Discussion

ZmRap2.7 is a novel gene regulating ABA signalling and seed vigour after accelerated ageing

The retention of seed vigour during storage is a key quality parameter for commercial seed lots, and also the most important trait relating to the conservation of germplasm resources (Reed et al., 2022; Zhou et al., 2020). Seed vigour changes during storage are greatly related to the deterioration process, which involves many biochemical changes relating to protective compounds, including intracellular integrity, enzyme activity, lipid peroxidation and ROS scavenging (Zhou et al., 2020). Dozens of genes relating to such changes have been identified to regulate seed vigour during storage. For example, *VITAMIN E1* (*VTE1*), *VTE2*, *Aldo-Ketoreductase 1* (*AKR1*) and *Lipoxygenase* (*LOX*) could reduce the production of lipid peroxidation to enhance seed longevity in Arabidopsis and rice (Nisarga et al., 2017; Sattler et al., 2004; Xu et al., 2015; Zhou et al., 2020). Protein L-isoaspartyl methyltransferase gene *PIMT* and methionine sulfoxide reductases gene *MSR* involved in protein repair, and
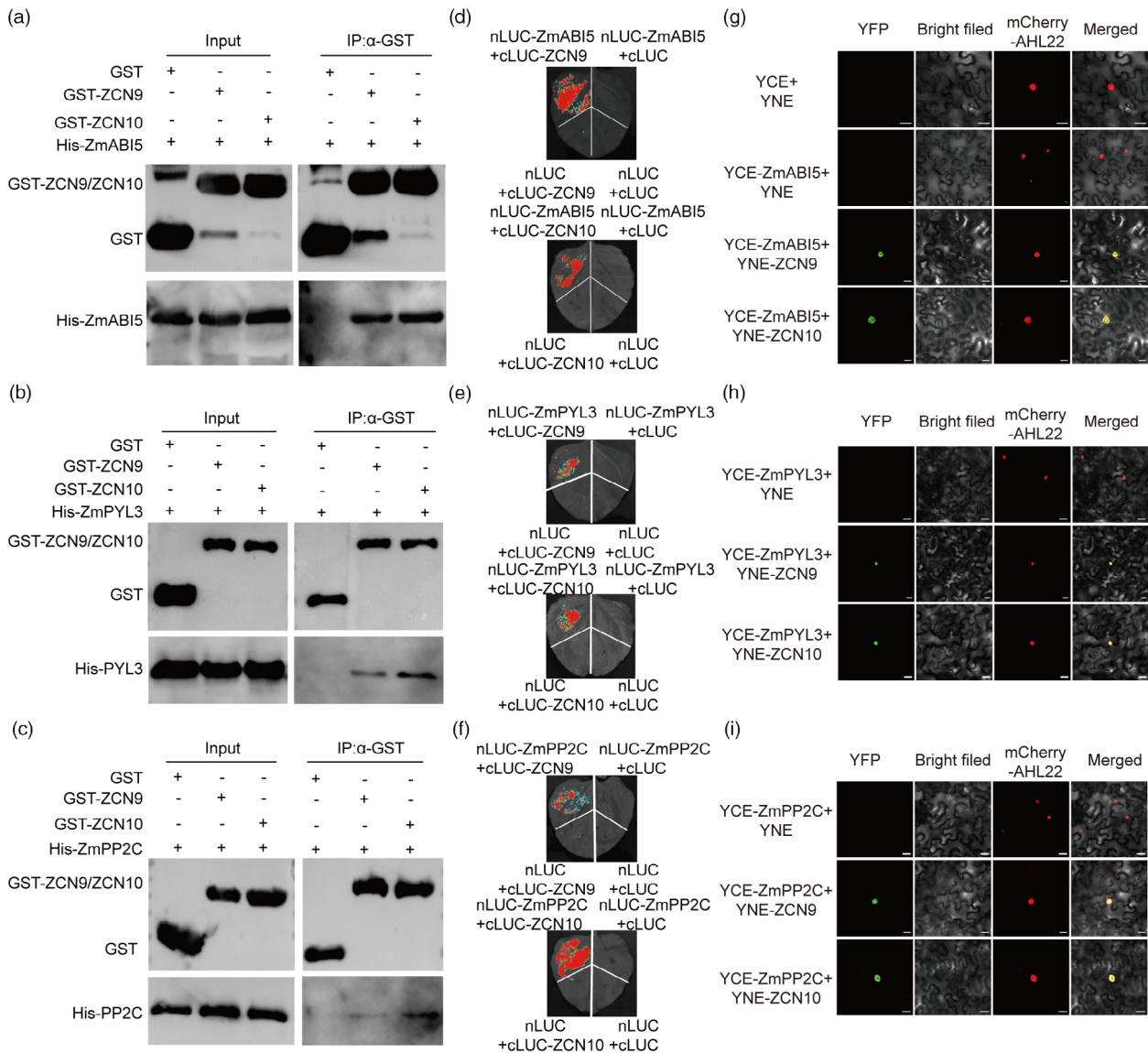
Figure 5 ZCN9 and ZCN10 interact with ZmPYL3, ZmPP2C and ZmABI5. (a–c) Pull-down assays showing that ZCN9 and ZCN10 interact with ZmABI5 (a), ZmPYL3 (b) and ZmPP2C (c). Recombinant proteins were immunoprecipitated with an anti-GST antibody and then immunoblotted using either anti-GST (upper part) or anti-His (lower part) antibody. (d–f) Luciferase complementation imaging (LCI) assays showing that ZCN9 and ZCN10 interact with ZmABI5 (d), ZmPYL3 (e) and ZmPP2C (f) in *N. benthamiana* leaves. (g–i) Bimolecular fluorescence complementation (BiFC) assays showing that ZCN9 and ZCN10 interact with ZmABI5 (g), ZmPYL3 (h) and ZmPP2C (i) in *N. benthamiana* leaves. The fluorescence signals represent the interaction activities and mcherry-AHL22 is the nucleus maker. Bar = 20 μm.

DNA glycosylase gene *OGG1* encoded protein to repair DNA damage during seed deterioration (Châtelain *et al.*, 2013; Ogé *et al.*, 2008; Waterworth *et al.*, 2010, 2016; Zhang *et al.*, 2023). Moreover, rice *1-CYS PEROXIREDOXIN* (*PER1*) was regarded as a seed-specific antioxidant to maintain high seed vigour by scavenging ROS (Wang *et al.*, 2022a). In maize, galactinol and raffinose synthase-related genes *GLOS* and *RS* functioned in energy storage and release and could enhance seed vigour through the RFOs biosynthesis (Li *et al.*, 2017).

ABA is a vital hormone in regulating seed germination, usually acting as an upstream regulator (Sybilska and Daszkowska-Golec, 2023). Previous works identified three *ABF* genes, *ABI3* to *ABI5*, from Arabidopsis, and found that *ABI3* (a B3 transcription factor) functions in upstream of *ABI5* (a bZIP transcription factor)

and both transcriptionally regulate genes in biochemical processes relating to LEA and RFOs during seed AA germination (Mao and Sun, 2015; Zinsmeister *et al.*, 2016). ABI4 (an AP2 transcription factor) could directly target the *PIMT* gene to improve protein repair ability during seed storage (Kamble *et al.*, 2022). In rice, ABA promoted bZIP23 could transcriptionally activate *OsPER1A* expression and involve in controlling of peroxiredoxin pathway during aged germination (Wang *et al.*, 2022a). In maize, ZmVP1 (an orthologous protein of AtABI3) interacts with ZmABI5 and regulates *ZmGOLS2* expression and raffinose accumulation in seeds for regulating vigour (Zhang *et al.*, 2019). These results indicated that ABA signalling is essential for seed-aged germination, which might be through its functions of regulating accumulation of protective proteins and

protein-repairing proteins during storage. Although the functions of ABA in seed vigour have been intensively investigated, the upstream regulators of ABA were largely unknown.

In this study, we characterized an AP2 transcription factor, ZmRap2.7, with an essential function in regulation of seed vigour from maize. Evidence showed that *ZmRap2.7* is highly expressed in embryo, and its loss-of-function mutants decreased seed

AA-GP, suggesting it as a positive regulator for seed vigour (Figure 2). Furthermore, Y1H and EMSA results showed that ZmRap2.7 could bind to promoters of three ABA signalling genes, *ZmPYL3*, *ZmPP2C* and *ZmABI5* (Figure 3). The GAL4 system revealed that ZmRap2.7 could repress expression of the report gene LUC (Figure 6e). Together with increased expressions of the three ABA signalling genes and decreased sensitivity to ABA
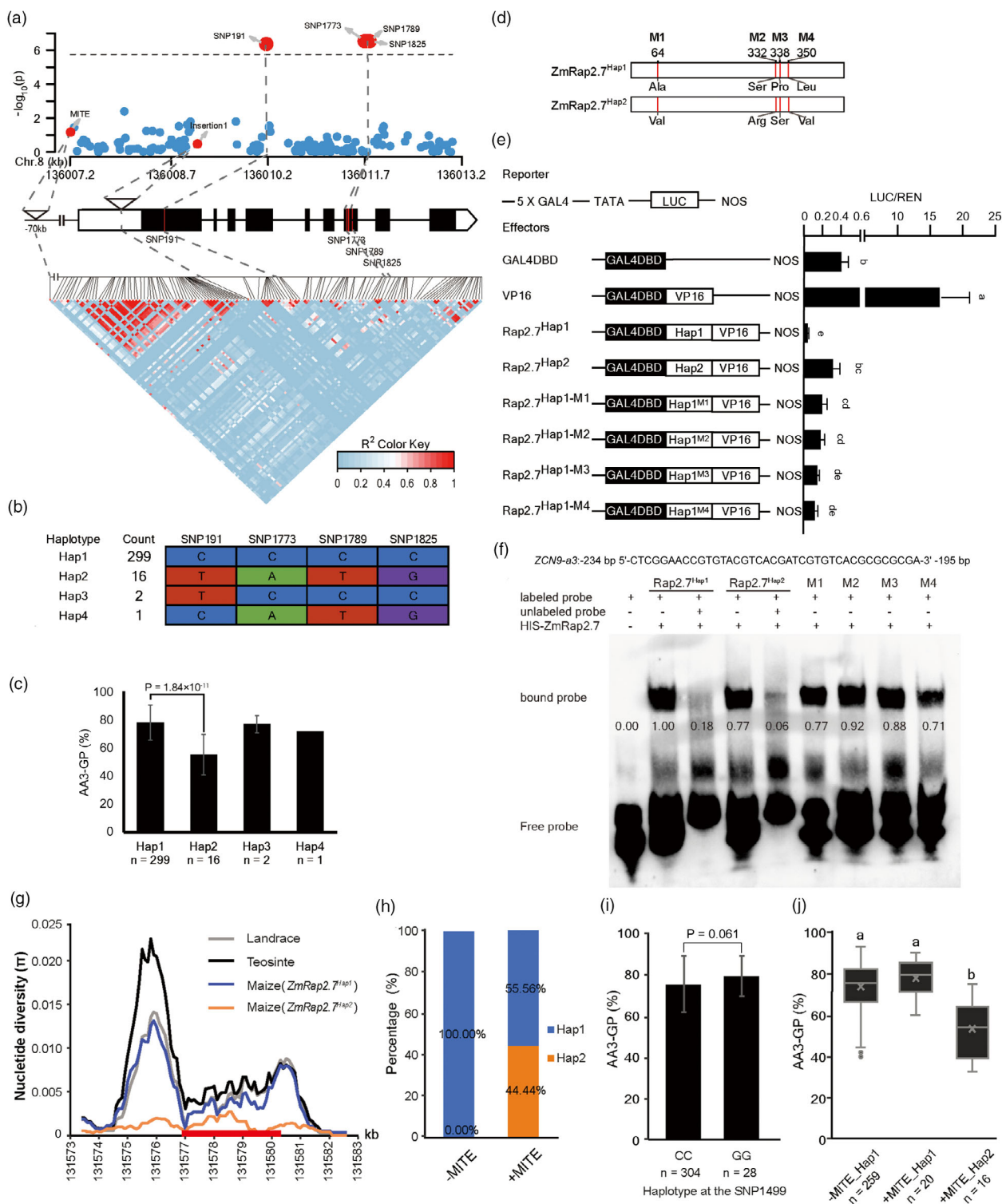

© 2024 The Authors. *Plant Biotechnology Journal* published by Society for Experimental Biology and The Association of Applied Biologists and John Wiley & Sons Ltd., 1–16

Figure 6 Allelic variation and evolution of *ZmRap2.7* in seed vigour regulation. (a) *ZmRap2.7*-based association mapping and pairwise LD analysis according to the B73 reference genome (Zm-B73-REFERENCE-GRAMENE-4.0). Triangles denote InDels, and dots represent SNPs. Exons and untranslated regions are shaded with black and white boxes respectively. The promoter and introns are shown as lines. (b) Haplotypes of *ZmRap2.7* identified in the AM368 panel of natural variants. 'count' denotes the number of germplasms in each haplotype group. (c) The comparison of 3-day accelerated ageing germination percentage (AA3-GP) between different haplotypes. (d) The schematic diagram of amino acid changes between Hap1 and Hap2. (e) A luciferase assay comparing the binding activity of different haplotypes in maize protoplasts. 5 × GAL4, multimerized GAL4 binding site; GAL4DBD, DNA-binding site of the GAL4 protein; M1–M4, the four SNPs mutations in the Hap1 background; Nos, nopaline synthase terminator; TATA, TATA box; VP16, strong activation domain from VP16 of the herpes simplex virus. The relative luciferase (LUC) activity is represented by the ratio of signal values of the firefly LUC to that of the Renilla LUC (internal control). Data are shown as the means of three independent transformants. Different lowercase letters indicate significant differences by Duncan's test ($P < 0.05$). (f) EMSA assays showing the transcription binding activities of Hap1, Hap2 and the four SNP mutated (M1–M4) ZmRap2.7 proteins on *ZCN9* promotor *in vitro*. (g) Nucleotide diversity for the genomic region of *ZmRap2.7* in teosinte, landrace and maize. The region includes gene body, 4-kb upstream and 3-kb downstream of *ZmRap2.7*. The red line indicates *ZmRap2.7* gene body. (h) The proportions of *ZmRap2.7^{Hap1}* and *ZmRap2.7^{Hap2}* lines in lines with and without MITE insertion. (i) The comparison of AA3-GP between lines with variants associated with brace root development (haplotype CC and GG). Different letters indicate significant differences between different groups. (j) The comparison of AA3-GP among −MITE+Hap1, +MITE+Hap1 and +MITE-Hap2 lines.

treatment in *ZmRap2.7* KO lines (Figure 3), it concluded that *ZmRap2.7* functioned in upstream of ABA for repressing its signalling by binding three signalling gene promoters during seed AA germination. We conducted a luciferase assay using pGreenII0800 system in protoplasts, but only found that the LUC activity driven by *ZmPP2C* and *ZmABI5* promoters could be repressed by ZmRap2.7 protein, whereas the activity driven by *ZmPYL3* promoter showed increased activity (Figure S19). As the protoplast was extracted from mesophyll cell protoplasts, where the inner cellular environments, such as some co-factors, might differ from that in seed cells, this result might indicate a complex repressing mechanism of *ZmRap2.7* on ABA signalling.

ZCN9 and ZCN10 might be novel cofactors regulating ABA signalling and seed vigour after accelerated ageing

PEBP are highly conserved proteins with diverse biological functions in animals and plants that act as modulators of intracellular signalling pathways (Danilevskaya *et al.*, 2008; Zhu *et al.*, 2021). In plants, PEBP family is generally divided into three subfamilies, FT-like, MFT-like and TFL1-like (Danilevskaya *et al.*, 2008). *FT-like* and *TFL1-like* genes are usually involved in the flowering time regulation, such as the famous florin gene *FT* in Arabidopsis and its ortholog *ZCN8* in maize (Danilevskaya *et al.*, 2008). Unlike the other two subfamilies, *MFT-like* genes expressed exclusively in seed and participated in regulating seed germination and dormancy in Arabidopsis, rice and wheat (Nakamura *et al.*, 2011; Song *et al.*, 2020; Xi *et al.*, 2010). In this study, we identified two new MFT-like members, *ZCN9* and *ZCN10*, whose expressions are exclusive in seed and increased by *ZmRap2.7* knockout (Figure 4a). Together with the fact that their promoters can be bound by ZmRap2.7 protein (Figure 4c,d), it indicated that *ZCN9* and *ZCN10* expressions could also be transcriptionally repressed by ZmRap2.7, a phenomenon same to the *ZmPYL3*, *ZmPP2C* and *ZmABI5* expressions. However, unlike the decreased promoter activities of *ZmPP2C* and *ZmABI5*, *ZCN9* and *ZCN10* promoter activities increased after adding ZmRap2.7 protein in the leaf protoplast (Figure S19), which is inconsistent with their increased expressions in *ZmRap2.7* KO lines. As *ZCN9* and *ZCN10* are seed-specific expression genes, this inconsistency is probably due to the different inner cell environments between leaf cells and seed cells. Together, these results identified an upstream regulator for *MFT*-like gene expressions, which extended the understanding of regulation of *MFT*-like subfamily gene expressions in crops.

Previous works revealed that the MFT-like proteins could interact with ABF proteins to regulate seed germination. For example, the Arabidopsis MFT protein, a homologue of ZCN9 and ZCN10, was found to interact with ABI5 protein and inhibit *ABI5* expression (Xi *et al.*, 2010). The rice OsMFT2 interacts with three bZIP transcription factors to enhance their binding to the downstream ABA-responsive genes (Song *et al.*, 2020). Here, we not only observed the interaction between ZCN9/10 and ABF proteins ZmABI5 but also found that ZCN9/10 interacted with ZmPYL3 and ZmPP2C proteins, two other members in ABA signalling (Figure 5). Moreover, *ZCN9* overexpression decreased *ZmRap2.7*, *ZmABI5* and *ZmPYL3* expression levels, indicating that *ZNC9* could further regulate expressions of its upstream gene (*ZmRap2.7*) and its interaction genes (*ZmABI5* and *ZmPYL3*) through some unknown mechanism (Figure S20). Thus, these results suggested that *ZCN9/ZCN10* regulating seed vigour might be through the functions as modulators for regulating ABA signalling by interacting with signalling proteins, as well as by regulating expressions of signalling genes and signalling upstream genes. However, it cannot exclude the possibility that *ZCN9* and *ZCN10* involves in pathways other than ABA signalling for regulating seed vigour. Future research will be interesting to uncover the comprehensive network relating to *ZCN9/ZCN10* mediated seed vigour regulation.

Pleiotropy of *ZmRap2.7* in regulating seed vigour and other traits

Pleiotropy is a common phenomenon in plants, particularly for the important agronomic traits controlling genes (Hendelman *et al.*, 2021; Song *et al.*, 2022). For example, the classical gene *OsIPA1* could promote both yield and disease resistance by targeting different downstream genes in rice (Song *et al.*, 2022; Wang *et al.*, 2018). However, unlike *IPA1*, pleiotropy of most genes was usually antagonistic, which makes their breeding application challenging in crops (Auge *et al.*, 2019; Khaipho-Burch *et al.*, 2023; Smith, 2016). Therefore, it is generally interesting to uncover their molecular mechanism responding to pleiotropy.

ZmRap2.7 was firstly reported to act as the functional gene of the important QTL, *Vgt1*, to negatively regulate flowering time in maize (Salvi *et al.*, 2007). Later, *ZmRap2.7* was found to regulate brace root development (Li *et al.*, 2019a). In this study, we demonstrated the third function of *ZmRap2.7* in positively regulating seed vigour. The pleiotropy of *ZmRap2.7* had also been supported by a combination analysis of 162 distinct traits
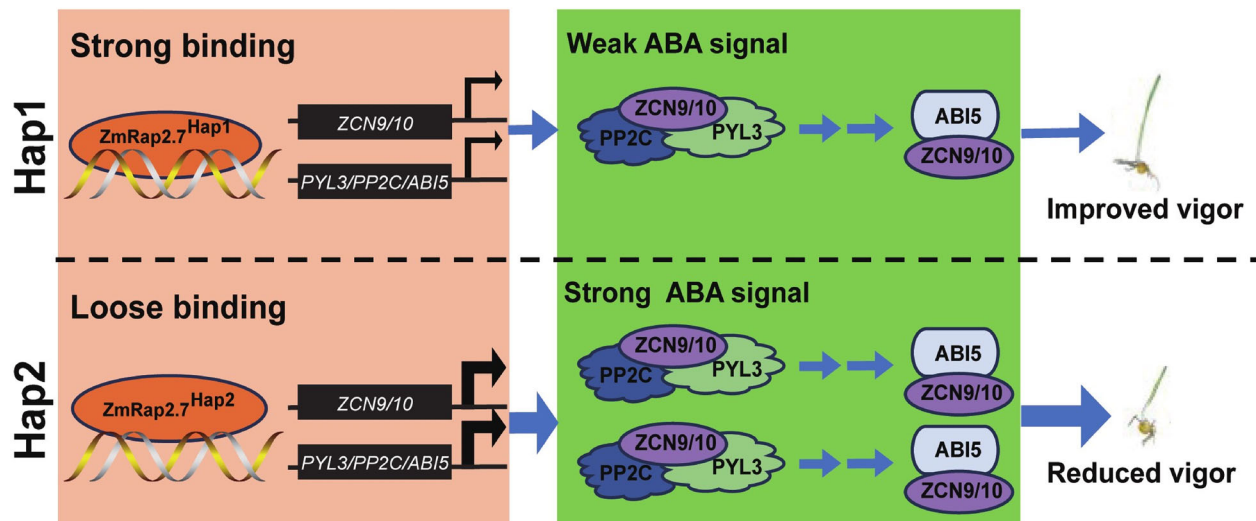
Figure 7 A proposed working model for *ZmRap2.7* in regulating seed vigour in maize. ZmRap2.7 transcriptionally represses expressions of *ZCN9* and *ZCN10*, and three ABA signalling genes *ZmPYL3*, *ZmPP2C* and *ZmABI5*. ZCN9/10 could interact with the three ABA signalling proteins to be involved in ABA signalling. The two haplotypes of *ZmRap2.7* influence its transcriptionally binding activity on the downstream gene and regulate ABA signalling mediated seed vigour.

within three diverse association panels, where *ZmRap2.7* locus is associated with a peak consisting of 13 SNPs that were detected for flowering traits and a number of vegetative traits (Mural *et al.*, 2022). Moreover, *ZmRap2.7* ortholog in Arabidopsis was the floral transition inhibitor *TOE1* (Aukerman and Sakai, 2003). This gene also showed pleiotropic functions in regulation of flowering time (Zhang *et al.*, 2015), innate immunity (Zou *et al.*, 2018), abaxial trichomes (Liu *et al.*, 2023) and root regeneration (Wang *et al.*, 2022b). An upstream transcription factor of *ZmRap2.7*, *ZmMADS69*, has been shown to associate with flowering traits and multiple vegetative traits (Liang *et al.*, 2019). Thus, these studies suggested that pleiotropy of *ZmRap2.7* and its orthologs might commonly exist in plants, and it will be interesting to uncover the mechanism responding to different functions.

The MITE insertion into *Vgt1* locus inhibited *ZmRap2.7* expression in cis-form and alleviated the inhibition of *ZmRap2.7* on maize flowering stage (Castelletti *et al.*, 2014). The SNP1499 in *ZmRap2.7* gene body responded to brace root development (Li *et al.*, 2019a). It was interesting to find that the MITE insertion did not relate to brace root development, and the SNP1499 was not relevant to flowering time (Castelletti *et al.*, 2014). In this study, we identified four SNPs located in *ZmRap2.7* coding region showing different transcriptionally repressing activity to its target gene *ZCN9* and *ZCN10* expressions (Figure S15), which responded to the divergence of seed vigour in this population. Further results supported that these four SNPs were not related to either flowering time or brace root development (Figure S17, S18). Meanwhile, both MITE insertion and SNP1499 were not related to seed vigour (Figure 6i,j). These results suggested that the distinct allelic variations of *ZmRap2.7* could be supposed to regulate flowering time, brace root development and seed vigour independently.

To explore the possible evolutional achievement of these distinct allelic variations within *ZmRap2.7*, we downloaded HapMap 3 data, which contained genome sequences for 18 teosinte, 24 landrace and 1034 improved maize (Bukowski

et al., 2018). Together with the genome sequences of the AMP368 panel, we found that the four seed vigour associated SNP only existed in maize lines with the MITE insertion (Figure 6h), while the root-associated SNP1499 only existed in lines without the MITE insertion (Figure S16), indicating that the MITE insertion may be selected firstly during domestication, and then different SNPs located in gene coding region were selected to depress seed vigour and improve brace root development independently in MITE insertion lines and none-insertion lines respectively.

In summary, this study characterized that *ZmRap2.7*, a previously identified AP2 transcription factor with functions in regulating flowering time and brace root development, positively regulates seed vigour by transcriptionally repressing expressions of *ZCN9* and *ZCN10*, and three ABA signalling genes *ZmPYL3*, *ZmPP2C* and *ZmABI5* (Figure 7). Moreover, ZCN9/10 could further interact with the three ABA signalling proteins to involve in ABA signalling (Figure 7). Four SNPs in *ZmRap2.7* coding region could influence its transcriptionally binding activity on the downstream gene promoters (Figure 7), but not relevant to flowering time and brace root development.

Experimental procedures

Phenotyping of seed accelerated ageing vigour

The AMP368 was planted in Sanya, Hainan province in the winter of 2011, 2016 and 2017. SG test was conducted in paper row system according to the methods from International Seed Testing Association (ISTA, 2015). The GP was scored 7 days after sowing, which was expressed as the ratio of germinated seeds to the total tested seeds. AA treatment was conducted by putting seeds in an ageing box for 3 or 6 days under 45 °C and 100% humidity condition. After AA treatment, seeds were air-dried until water content dropped to 14%, and then used for SG test. For ABA treatment, aged seeds were sowed in sand, and were moisturized with 16% water with or without 300 mM ABA. After 7 days, GP were evaluated. For phenotyping, three independent replicates were conducted with 30 seeds for each replicate.

Genome-wide association study

GWAS is executed in the Tassel 5.2.81 (Fu et al., 2013). Population structure matrix and kinship matrix were input into mixed linear model (MLM) to control for false positives in association analysis and ($-\log_{10}$ (P) $\geq -\log_{10}$(1/effective SNP number (EN)); EN=533906)) was used as a threshold. Phenotypic variation explained rates were calculated using lm function package.

ZmRap2.7-based association analysis

The resequencing data of 358 maize inbred lines belonging to the 368 population were obtained from Genome Sequence Archive (GSA, https://ngdc.cncb.ac.cn/gsa/browse/CRA001363) and aligned to the reference genome sequence (B73, AGPv4). SNPs that had missing values greater than 20% and minor allele frequency (MAF) <5% were removed from further analysis. Totally, 177 SNPs from 2-kb upstream and 1-kb downstream of *ZmRap2.7* were used for association analysis. Moreover, we re-sequenced *ZmRap2.7* genome sequence and found a presence/absence variation (PAV) in 813 bp upstream of the ATG. Together with the classical MITE element in ~70-kb upstream of ZmRap2.7 (Castelletti et al., 2014) and the PAV, candidate gene association was carried out using the method same as GWAS.

Quantitative RT–PCR analysis and *in situ* hybridization

Total RNA extraction, the first-strand cDNA synthesis and qPCR processing were conducted as previously described (Chen et al., 2021). The quantification method ($2^{-\Delta Ct}$) was used to calculate gene expression with three biological replicates. The maize *GAPDH* gene was used as an internal control. The primers are listed in Table S3.

The immature seeds were harvested 18 days after pollination (DAP), and fixed in 3.7% FAA solution for *in situ* hybridization following a method described previously (Chen et al., 2021), with hybridization probe sequences listed in Table S3.

Transgenic maize construction

The open reading frame (ORF) of ZCN9 and ZCN10 was amplified from germinated embryo of B73 using primers listed in Table S3 and inserted into the pCambia3301 vector driven by a ubiquitin promoter. The constructed vectors were transformed into immature embryos of maize inbred line CAL according to the *Agrobacterium*-mediated transformation method using *Agrobacterium* strain LBA4404. The positive and WT plants were identified using PCR analysis with primers in Table S3.

Transcriptome sequencing

Fifty embryos from each sample of 24-h AA3 germinated seeds were harvested with three replications, ground in liquid nitrogen and used for RNA extraction (Tiangen, Beijing, China). Total RNA was used to construct a library and perform RNA sequencing with a read length of 150 bp (pared end) using the Illumina platform (Annoroad, Beijing, China). Clean reads were obtained by Perl scripts processing, and then mapped to the reference genome (B73, AGPv4) using the HISAT2 program (Anders et al., 2015). DESeq2 package was used for the identification of DEGs with a threshold of $P < 0.05$ and $\log_{2}$(|fold change|) $\geq$1 (Love et al., 2014). FPKM (expected number of fragments per kilobase of transcript sequence per millions of base pairs sequenced) is used for estimating gene expression levels. Cufflinks were employed to assemble the transcripts, estimate their abundances and test for differential expressions in RNA-Seq samples (Trapnell et al., 2012). The agriGO online website (http://systemsbiology. cau.edu.cn/agriGOv2/) was used to perform gene ontology analysis under a threshold of FDR < 0.05.

Yeast one-hybrid and yeast two-hybrid assay

The Y1H assays were performed as described previously (Qi et al., 2020). Gene promoters were amplified from B73 and introduced into the Placzi vector. The AD-fusion expression plasmids containing *ZmRap2.7* ORF or the PB42AD empty vector were transformed together with the Placzi-promoter vector into yeast strain EGY48. Yeast transformants were applied to an SD/−Trp-Ura solid medium and cultured at 30 °C for 3 days, and then bred on SD/Gal/Raf-Trp-Ura solid medium including X-Gal (5-bromo-4-chloro-3-indolyl-b-D-galactopyranoside) for blue colour development.

For Y2H analysis, the ORFs of *ZmPYL3*, *ZmPP2C* and *ZmABI5* were cloned into pGADT7 vector, and the ORFs of *ZCN9* and *ZCN10* were cloned into pGBDKT7 vector. Each pair of the pGADT7 and pGBKT7 fusion vectors was co-transformed into yeast strain Mav203. The transforms were grown on a selective medium lacking Leu and Trp (SD/−Leu-Trp), then transferred to an SD/−Leu-Trp-His-Ade medium containing 3-amino-1,2,4-triazole (3-AT) as a competitive inhibitor of the HIS3 product. Finally, X-α-gal was supplemented for blue colour development. Protein interactions were observed after 3 days of growth at 30 °C.

Luciferase complementation image (LCI)

The LCI assay with the pCAMBIA1300-nLUC and pCAMBIA1300-cLUC vectors was conducted as described previously (Chen et al., 2008). The *ZCN9* and *ZCN10* ORFs were cloned to pCAMBIA1300-cLUC, and *ZmPYL3*, *ZmPP2C* and *ZmABI5* ORFs were cloned to pCAMBIA1300-nLUC. *Agrobacterium strain* GV3101 containing infused nLUC and cLUC vectors was co-infiltrated into tobacco leaves. After 2-day infiltration, luciferin (100 mM) was used on the leaf surface in the dark, and luciferase signals were detected using VILBER FUSION FX7 Spectra (VILBER, Paris, France).

Bimolecular fluorescence complementation assay (BiFC)

The ORFs of *ZmABI5*, *ZmPYL3* and *ZmPP2C* were recombined into the pSPYNE-35S vector containing nYFP, and ORFs of *ZCN9* and *ZCN10* into the pSPYCE-35S vector containing cYFP. *Agrobacterium strain* GV3101 containing infused nYFP and cYFP vectors was co-infiltrated into tobacco leaves. After 48 h, the fluorescence signals were detected using a confocal laser-scanning microscope (LSM880; Zeiss, Oberkochen, Germany).

Electrophoretic mobility shift assay (EMSA)

The ORF of *ZmRap2.7* was cloned into the pET30a vector and transformed into the *Escherichia coli* strain BL21. The recombinant protein was enriched with IPTG induction at 16 °C for 20 h, and purified using His-tag Protein Purification beads (Thermo Fisher Scientific, Waltham). The biotin-labelled complementary oligonucleotides were synthesized by Sangon (Sangon Biotech Co., Ltd, Shanghai, China) and formed double-stranded probes by heating for 5 min at 100 °C and cooling slowly at room temperature. The probe sequences are listed in Table S3.

EMSA assays were performed using a Light Shift Chemiluminescent EMSA kit (Thermo Fisher Scientific, Waltham) following the manufacturer's instruction. The purified protein and

biotin-label probe were incubated together at 25° for 20 min. The binding products were separated by electrophoresis on 6% native-PAGE gel, and then pre-electrophoresed for 1 h. Then, the samples were transferred to nylon membrane at 380 mA for 45 min, and the chemiluminescence was detected using Chemi-Scope6100 (CliNX, Shanghai, China).

Dual-luciferase transcriptional activity assay

The ORF of *ZmRap2.7^{Hap1}*, *ZmRap2.7^{Hap2}* and four mutations of *ZmRap2.7^{Hap1}*(M1–M4) were cloned into the GAL4DBD vector driven by the CaMV 35S promoter, acting as effector vectors. The strong activation domain from viral protein16 (VP16) of the herpes simplex virus was fused to either N or C terminus of *ZmRap2.7* ORF to elevate the LUC activity. The GAL4DBD empty vector with and without VP16 was regarded as negative control and positive control respectively. The luciferase vector with 5 × GAL4 binding site in upstream of LUC reporter gene and the luciferase vector with Renilla LUC were used as reporter vectors.

For the pGreenII0800 system, the full-length ORF of *ZmRap2.7* was cloned into the effector vector pGreenII 62-SK under the control of the CaMV 35S promoter. The ~1.5 kb promoter fragment of *ZCN9/10*, *ZmPYL3*, *ZmPP2C* and *ZmABI5* was cloned into the reporter vector pGreenII0800-LUC. CaMV35S promoter-driven REN was used as an internal control.

The reporter vector and the effector vector were co-transformed into maize mesophyll cell protoplasts, which were cultured at 25 °C for 14 h in the dark. The transformed protoplasts were enriched by centrifugation, and then cleaved by adding a passive lysis buffer (PLB, Shanghai, China). The luciferase activity was measured using the Dual-Luciferase Reporter Assay System (Promega, Shanghai, China) following the manufacturer's instruction. The substrate luciferin was added and catalysed by luciferase to emit fluorescence (the strongest wavelength was around 560 nm). The firefly luciferase activity was recorded immediately, and the Renilla luciferase activity was measured after adding Stop & Glo® Reagent. The ratio of the firefly luciferase value to the Renilla luciferase value was calculated with four biological replicates.

Evolution analysis of *ZmRap2.7* haplotypes

Maize HapMap 3 data downloaded from https://www.panzea.org/ were used to calculate the nucleotide diversity along 5-kb upstream to 5-kb downstream region of *ZmRap2.7* (Bukowski et al., 2018). The function sliding.window.transform of R package POPGENOME (Pfeifer et al., 2014) was used to generate sliding windows (window size = 1000 bp, step size = 100 bp). Nucleotide diversity (P) in each sliding window was calculated for maize, landrace and teosinte (*Zea may* ssp. parviglumis) using the function diversity.stats. Classification of maize is based on the genotypes of the lead SNP (chr8.S_132046298), which is most significantly associated with AA3-GP.

The flowering time of heading date, pollen shed time and silking time were downloaded from maizego website (http://www.maizego.org/), and the brace root numbers were extracted from Li et al. for the AMP368 panel (Li et al., 2019a).

Accession numbers

The datasets generated and/or analysed during the current study are provided in this paper. The transcriptome sequencing data are available at Genome Sequence Archive (GSA, https://ngdc.cncb.ac.cn/gsa/) with accession number subCRA020522.

Conflict of interest

The authors declare no competing interests.

Author contributions

G.R., D.X. and W.J. designed experiments. G.S. and A.J. performed most of the experiments. D.X., G.R., G.S. and A.J. wrote the manuscript. A.J., Z.N., Z.H. and P.Q. analysed the data. H.H., X.Z., C.Q., L.L., L.Y., L.J., C.F. and F.J. interpreted the results.

Data availability statement

The datasets generated and/or analyzed during the current study are provided with this paper. The transcriptome sequencing data are available at Genome Sequence Archive (GSA, https://ngdc.cncb.ac.cn/gsa/) with accession number subCRA020522.

References

Anders, S., Pyl, P.T. and Huber, W. (2015) HTSeq—a Python framework to work with high-throughput sequencing data. *Bioinformatics* **31**, 166–169.

Auge, G.A., Penfield, S. and Donohue, K. (2019) Pleiotropy in developmental regulation by flowering-pathway genes: is it an evolutionary constraint? *New Phytol.* **224**, 55–70.

Aukerman, M. and Sakai, H. (2003) Regulation of flowering time and floral organ identity by a MicroRNA and its APETALA2-like target genes. *Plant Cell* **15**, 2730–2741.

Bueso, E., Muñoz-Bertomeu, J., Campos, F., Brunaud, V., Martínez, L., Sayas, E., Ballester, P. et al. (2013) *ARABIDOPSIS THALIANA HOMEOBOX25* uncovers a role for gibberellins in seed longevity. *Plant Physiol.* **164**, 999–1010.

Bukowski, R., Guo, X., Lu, Y., Zou, C., He, B., Rong, Z., Wang, B. et al. (2018) Construction of the third-generation *Zea mays* haplotype map. *Gigascience* **7**, 1–12.

Castelletti, S., Tuberosa, R., Pindo, M. and Salvi, S. (2014) A MITE transposon insertion is associated with differential methylation at the maize flowering time QTL *Vgt1*. *G3-Genes Genom. Genet* **4**, 805–812.

Châtelain, E., Satour, P., Laugier, E., Vu, B., Payet, N., Rey, P. and Montrichard, F. (2013) Evidence for participation of the methionine sulfoxide reductase repair system in plant seed longevity. *Proc. Natl. Acad. Sci. USA* **110**, 3633–3638.

Chen, H., Chu, P., Zhou, Y., Ding, Y., Li, Y., Liu, J., Jiang, L. et al. (2016) Ectopic expression of *NnPER1*, a Nelumbo nucifera 1-cysteine peroxiredoxin antioxidant, enhances seed longevity and stress tolerance in Arabidopsis. *Plant J.* **88**, 608–619.

Chen, H., Zou, Y., Shang, Y., Lin, H., Wang, Y., Cai, R., Tang, X. et al. (2008) Firefly luciferase complementation imaging assay for protein-protein interactions in plants. *Plant Physiol.* **146**, 368–376.

Chen, Q., Zhang, J., Wang, J., Xie, Y., Cui, Y., Du, X., Li, L. *et al.* (2021) Small kernel 501 (smk501) encodes the RUBylation activating enzyme E1 subunit ECR1 (E1 C-TERMINAL RELATED 1) and is essential for multiple aspects of cellular events during kernel development in maize. *New Phytol.* **230**, 2337–2354.

Clerkx, E., Vries, H., Ruys, G., Groot, S. and Koornneef, M. (2003) Characterization of green seed, an enhancer of abi3-1 in Arabidopsis that affects seed longevity. *Plant Physiol.* **132**, 1077–1084.

Cutler, S., Rodriguez, P., Finkelstein, R. and Abrams, S. (2010) Abscisic acid: emergence of a core signaling network. *Annu. Rev. Plant Biol.* **61**, 651–679.

Danilevskaya, O., Meng, X., Hou, Z., Ananiev, E. and Simmons, C. (2008) A genomic and expression compendium of the expanded *PEBP* gene family from maize. *Plant Physiol.* **146**, 250–264.

Du, X., Fang, T., Liu, Y., Huang, L., Zang, M., Wang, G., Liu, Y. *et al.* (2019) Transcriptome profiling predicts new genes to promote maize callus formation and transformation. *Front. Plant Sci.* **10**, 1633.

Erenstein, O., Jaleta, M., Sonder, K., Mottaleb, K. and Prasanna, B. (2022) Global maize production, consumption and trade: trends and R&D implications. *Food Secur.* **14**, 1295–1319.

Fu, J., Cheng, Y., Linghu, J., Yang, X., Kang, L., Zhang, Z., Zhang, J. *et al.* (2013) RNA sequencing reveals the complex regulatory network in the maize kernel. *Nat. Commun.* **4**, 2832.

Han, Q., Chen, K., Yan, D., Hao, G., Qi, J., Wang, C., Dirk, L.M.A. *et al.* (2020) *ZmDREB2A* regulates *ZmGH3.2* and *ZmRAFS*, shifting metabolism towards seed aging tolerance over seedling growth. *Plant J.* **104**, 268–282.

Hendelman, A., Zebell, S., Rodriguez-Leal, D., Dukler, N., Robitaille, G., Wu, X., Kostyun, J. *et al.* (2021) Conserved pleiotropy of an ancient plant homeobox gene uncovered by cis-regulatory dissection. *Cell* **184**, 1724–1739.

Hu, Y., Li, S., Fan, X., Song, S., Zhou, X., Weng, X., Xiao, J. *et al.* (2020) *OsHOX1* and *OsHOX28* redundantly shape rice tiller angle by reducing *HSFA2D* expression and auxin content. *Plant Physiol.* **184**, 1424–1437.

International Seed Testing Association (ISTA) (2015) *International Rules for Seed Test*. Switzerland: Zurich.

Kamble, N.U., Ghosh, S., Achary, R.K. and Majee, M. (2022) Arabidopsis *ABSCISIC ACID INSENSITIVE4* targets *PROTEIN L-ISOASPARTYL METHYLTRANSFERASE1* in seed. *Planta* **256**, 30.

Khaipho-Burch, M., Ferebee, T., Giri, A., Ramstein, G., Monier, B., Yi, E., Romay, M. *et al.* (2023) Elucidating the patterns of pleiotropy and its biological relevance in maize. *PLoS Genet.* **19**, e1010664.

Li, J., Chen, F., Li, Y., Li, P., Wang, Y., Mi, G. and Yuan, L. (2019a) *ZmRAP2.7*, an AP2 transcription factor, is involved in maize brace roots development. *Front. Plant Sci.* **10**, 820.

Li, L., Wang, F., Li, X., Peng, Y., Zhang, H., Hey, S., Wang, G. *et al.* (2019b) Comparative analysis of the accelerated aged seed transcriptome profiles of two maize chromosome segment substitution lines. *PLoS One* **14**, e0216977.

Li, T., Zhang, Y., Wang, D., Liu, Y., Dirk, L.M.A., Goodman, J., Downie, A.B. *et al.* (2017) Regulation of seed vigor by manipulation of raffinose family oligosaccharides in maize and *Arabidopsis thaliana*. *Mol. Plant* **10**, 1540–1555.

Liang, Y., Liu, Q., Wang, X., Huang, C., Xu, G., Hey, S., Lin, H.-Y. *et al.* (2019) *ZmMADS69* functions as a flowering activator through the *ZmRap2.7-ZCN8* regulatory module and contributes to maize flowering time adaptation. *New Phytol.* **221**, 2335–2347.

Liu, Y., Yang, S., Khan, A.R. and Gan, Y. (2023) TOE1/TOE2 interacting with GIS to control trichome development in *Arabidopsis. Int. J. Mol. Sci.* **24**, 6698.

Liu, Y., Zhang, H., Li, X., Wang, F., Lyle, D., Sun, L., Wang, G. *et al.* (2019) Quantitative trait locus mapping for seed artificial aging traits using an F$_{2:3}$ population and a recombinant inbred line population crossed from two highly related maize inbreds. *Plant Breed.* **138**, 29–37.

Love, M.I., Huber, W. and Anders, S. (2014) Moderated estimation of fold change and dispersion for RNA-seq data with DESeq2. *Genome Biol.* **15**, 550.

Mao, Z. and Sun, W. (2015) Arabidopsis seed-specific vacuolar aquaporins are involved in maintaining seed longevity under the control of *ABSCISIC ACID INSENSITIVE 3. J. Exp. Bot.* **66**, 4781–4794.

Mural, R.V., Sun, G., Grzybowski, M., Tross, M.C., Jin, H., Smith, C., Newton, L. *et al.* (2022) Association mapping across a multitude of traits collected in diverse environments in maize. *GigaScience* **11**, giac080.

Nakamura, S., Abe, F., Kawahigashi, H., Nakazono, K., Tagiri, A., Matsumoto, T., Utsugi, S. *et al.* (2011) A wheat homolog of *MOTHER OF FT AND TFL1* acts in the regulation of germination. *Plant Cell* **23**, 3215–3229.

Nisarga, K., Vemanna, R., Chandrashekar, B., Rao, H., Vennapusa, A., Narasimaha, A., Makarla, U. *et al.* (2017) Aldo-ketoreductase 1 (AKR1) improves seed longevity in tobacco and rice by detoxifying reactive cytotoxic compounds generated during ageing. *Rice* **10**, 11.

Ogé L, Bourdais G, Bove J r m, Collet B, Godin B A, Granier F, Boutin J-P, Job D, Jullien M, and Grappin P. (2008) Protein repair l-isoaspartyl methyltransferase1 is involved in both seed longevity and germination vigor in *Arabidopsis. Plant Cell* **20**, 3022–3037.

Pfeifer, B., Wittelsbürger, U., Ramos-Onsins, S. and Lercher, M. (2014) PopGenome: an efficient swiss army knife for population genomic analyses in R. *Mol. Biol. Evol.* **31**, 1929–1936.

Qi, L., Liu, S., Li, C., Fu, J., Jing, Y., Cheng, J., Li, H. *et al.* (2020) PHYTOCHROME-INTERACTING FACTORS interact with the ABA receptors PYL8 and PYL9 to orchestrate ABA signaling in darkness. *Mol. Plant* **13**, 414–430.

Rajjou, L., Duval, M., Gallardo, K., Catusse, J., Bally, J., Job, C. and Job, D. (2012) Seed germination and vigor. *Annu. Rev. Plant Biol.* **63**, 507–533.

Reed, R.C., Bradford, K.J. and Khanday, I. (2022) Seed germination and vigor: ensuring crop sustainability in a changing climate. *Heredity* **128**, 450–459.

Saatkamp, A., Cochrane, A., Commander, L., Guja, L., Jimenez-Alfaro, B., Larson, J., Nicotra, A. *et al.* (2019) A research agenda for seed-trait functional ecology. *New Phytol.* **221**, 1764–1775.

Salvi, S., Sponza, G., Morgante, M., Tomes, D., Niu, X., Fengler, K.A., Meeley, R. *et al.* (2007) Conserved noncoding genomic sequences associated with a flowering-time quantitative trait locus in maize. *Proc. Natl. Acad. Sci. USA* **104**, 11376–11381.

Sattler, S., Gilliland, L., Magallanes-Lundback, M., Pollard, M. and DellaPenna, D. (2004) Vitamin E is essential for seed longevity and for preventing lipid peroxidation during germination. *Plant Cell* **16**, 1419–1432.

Smith, S. (2016) Pleiotropy and the evolution of floral integration. *New Phytol.* **209**, 80–85.

Song, S., Wang, G., Wu, H., Fan, X., Liang, L., Zhao, H., Li, S. *et al.* (2020) *OsMFT2* is involved in the regulation of ABA signaling-mediated seed germination through interacting with OsbZIP23/66/72 in rice. *Plant J.* **103**, 532–546.

Song, X., Meng, X., Guo, H., Cheng, Q., Jing, Y., Chen, M., Liu, G. *et al.* (2022) Targeting a gene regulatory element enhances rice grain yield by decoupling panicle number and size. *Nat. Biotechnol.* **40**, 1403–1411.

Sybilska, E. and Daszkowska-Golec, A. (2023) A complex signaling trio in seed germination: Auxin-JA-ABA. *Trends Plant Sci.* **28**, 873–875.

Tian, R., Wang, F., Zheng, Q., Niza, V., Downie, A. and Perry, S. (2020) Direct and indirect targets of the arabidopsis seed transcription factor ABSCISIC ACID INSENSITIVE3. *Plant J.* **103**, 1679–1694.

Trapnell, C., Roberts, A., Goff, L., Pertea, G., Kim, D., Kelley, D.R., Pimentel, H. *et al.* (2012) Differential gene and transcript expression analysis of RNA-seq experiments with TopHat and Cufflinks. *Nat. Protoc.* **7**, 562–578.

Wang, B., Zhang, Z., Fu, Z., Liu, Z., Hu, Y. and Tang, J. (2016) Comparative QTL analysis of maize seed artificial aging between an immortalized F$_2$ population and its corresponding RILs. *Crop J.* **4**, 30–39.

Wang, J., Zhou, L., Shi, H., Chern, M., Yu, H., Yi, H., He, M. *et al.* (2018) A single transcription factor promotes both yield and immunity in rice. *Science* **361**, 1026–1028.

Wang, W., Xu, D., Sui, Y., Ding, X. and Song, X. (2022) A multiomic study uncovers a bZIP23-PER1A-mediated detoxification pathway to enhance seed vigor in rice. *Proc. Natl. Acad. Sci. USA* **119**, e2026355119.

Wang, Y., Sun, L., Wang, R., Li, H. and Zhu, Z. (2022) The AP2 transcription factors TOE1/TOE2 convey Arabidopsis age information to ethylene signaling in plant de novo root regeneration. *Planta* **257**, 1.

Waterworth, W., Footitt, S., Bray, C., Finch-Savage, W. and West, C. (2016) DNA damage checkpoint kinase ATM regulates germination and maintains genome stability in seeds. *Proc. Natl. Acad. Sci. USA* **113**, 9647–9652.

Waterworth, W.M., Masnavi, G., Bhardwaj, R.M., Jiang, Q., Bray, C.M. and West, C.E. (2010) A plant DNA ligase is an important determinant of seed longevity. *Plant J.* **63**, 848–860.

Weiner, J., Peterson, F., Volkman, B. and Cutler, S. (2010) Structural and functional insights into core ABA signaling. *Curr. Opin. Plant Biol.* **13**, 495–502.

Xi, W., Liu, C., Hou, X. and Yu, H. (2010) *MOTHER OF FT AND TFL1* regulates seed germination through a negative feedback loop modulating ABA signaling in Arabidopsis. *Plant Cell* **22**, 1733–1748.

Xu, H., Wei, Y., Zhu, Y., Lian, L., Xie, H., Cai, Q., Chen, Q. *et al.* (2015) Antisense suppression of *LOX3* gene expression in rice endosperm enhances seed longevity. *Plant Biotechnol. J.* **13**, 526–539.

Xue, X., Du, S., Jiao, F., Xi, M., Wang, A., Xu, H., Jiao, Q. *et al.* (2021) The regulatory network behind maize seed germination: effects of temperature, water, phytohormones, and nutrients. *Crop J.* **9**, 718–724.

Yang, N., Liu, J., Gao, Q., Gui, S., Chen, L., Yang, L., Huang, J. *et al.* (2019) Genome assembly of a tropical maize inbred line provides insights into structural variation and crop improvement. *Nat. Genet.* **51**, 1052–1059.

Zhang, B., Wang, L., Zeng, L., Zhang, C. and Ma, H. (2015) Arabidopsis TOE proteins convey a photoperiodic signal to antagonize CONSTANS and regulate flowering time. *Genes Dev.* **29**, 975–987.

Zhang, H. and Ogas, J. (2009) An epigenetic perspective on developmental regulation of seed genes. *Mol. Plant* **2**, 610–627.

Zhang, Y., Song, X., Zhang, W., Liu, F., Wang, C., Liu, Y., Dirk, L.M.A. *et al.* (2023) Maize *PIMT2* repairs damaged 3-METHYLCROTONYL COA CARBOXYLASE in mitochondria, affecting seed vigor. *Plant J.* **115**, 220–235.

Zhang, Y., Sun, Q., Zhang, C., Hao, G., Wang, C., Dirk, L.M.A., Downie, A.B. *et al.* (2019) Maize VIVIPAROUS1 interacts with ABA INSENSITIVE5 to regulate GALACTINOL SYNTHASE2 expression controlling seed raffinose accumulation. *J. Agric. Food Chem.* **67**, 4214–4223.

Zhou, W., Chen, F., Luo, X., Dai, Y., Yang, Y., Zheng, C., Yang, W. *et al.* (2020) A matter of life and death: Molecular, physiological, and environmental regulation of seed longevity. *Plant Cell Environ.* **43**, 293–302.

Zhu, Y., Klasfeld, S. and Wagner, D. (2021) Molecular regulation of plant developmental transitions and plant architecture via PEPB family proteins: an update on mechanism of action. *J. Exp. Bot.* **72**, 2301–2311.

Zinsmeister, J., Lalanne, D., Terrasson, E., Chatelain, E., Vandecasteele, C., Vu, B., Dubois-Laurent, C. *et al.* (2016) ABI5 is a regulator of seed maturation and longevity in Legumes. *Plant Cell* **28**, 2735–2754.

Zinsmeister, J., Leprince, O. and Buitink, J. (2020) Molecular and environmental factors regulating seed longevity. *Biochem. J.* **477**, 305–323.

Zou, Y., Wang, S., Zhou, Y., Bai, J., Huang, G., Liu, X., Zhang, Y. *et al.* (2018) Transcriptional regulation of the immune receptor FLS2 controls the ontogeny of plant innate immunity. *Plant Cell* **30**, 2779–2794.

Supporting information

Additional supporting information may be found online in the Supporting Information section at the end of the article.

Figure S1 *ZmRap2.7* expression in embryo during seed standard germination.

Figure S2 Germination performance of the *ZmRap2.7-Mu* mutation line.

Figure S3 The relative expression levels of the ABA response genes in 24 h AA3 germinated embryos of *ZmRap2.7* knockout line (*KO#1*) and WT.

Figure S4 Yeast one-hybrid assays between ZmRap2.7 protein and ABA signaling gene promoters.

Figure S5 Standard germination of *ZmRap2.7* knockout (KO) lines in response to ABA treatment.

Figure S6 Expression level of *ZmRap2.7* in B73 inbred line at 24 h after imbibition of AA3 germinated embryos with ABA treatment.

Figure S7 Expression of *ZCN11* gene in wild type (WT) and *ZmRap2.7* knockout line (*KO#1*).

Figure S8 Synteny analysis of maize *ZCN* genes and their Poaceae homologs in rice, sorghum and Brachpodium.

Figure S9 Expression patterns of *ZCN9* and *ZCN10*.

Figure S10 EMSA assays of ZmRap2.7 protein binding to different segments of *ZCN9* and *ZCN10* promoters *in vitro*.

Figure S11 Germination performance of *ZCN9* (a) and *ZCN10* (b) overexpression (OE) lines in response to ABA treatment.

Figure S12 *ZmRap2.7* expression in AA3 germinated embryos of randomly selected 53 Hap1 lines and the 16 Hap2 lines.

Figure S13 A luciferase assay comparing binding activity of ZmRap2.7 with the N and C terminus of the strong activation domain from viral protein16 (VP16).

Figure S14 The expressions of *ZCN9*, *ZCN10*, *ZmPYL3*, *ZmPP2C* and *ZmABI5* in AA3 germinated embryos of randomly selected 15 Hap1 lines and the 10 Hap2 lines.

Figure S15 EMSA assays of ZmRap2.7^{Hap1} and ZmRap2.7^{Hap2} proteins binding to *ZCN9* (a) and *ZCN10* (b) promoter segments *in vitro*.

Figure S16 The percentage of brace root associated haplotype (CC and GG) in lines with and without MITE element.

Figure S17 Comparison of heading date (a), pollen shedding time (b) and silking time (c) among -MITE+Hap1, +MITE+Hap1 and +MITE-Hap2 lines.

Figure S18 The comparison on number of brace root between lines with variants associated to seed vigor (Hap1 and Hap2).

Figure S19 A dual-luciferase assay showing binding activity of ZmRap2.7 on its target gene *ZCN9*, *ZCN10*, *ZmPYL3*, *ZmPP2C* and *ZmABI5*.

Figure S20 Expression levels of *ZmRap2.7*, *ZmPYL3*, *ZmPP2C* and *ZmABI5* in AA3 germinated embryos at 24 h after imbibition with ABA treatment in WT and *ZCN9* overexpressed lines.

Table S1 Statistical Analysis of accelerated aging germination percentage in an association population grown in three years.

Table S2 SNPs significantly associated with seed longevity.

Table S3 Primers used in this study.

Table S4 Significantly differentially expressed genes of ZmRap2.7-KO#1 compared with WT at 24 h after AA3 germination.

Table S5 The genotype of tested teosinte accessions and landraces.